

# Fully stochastic trust-region methods with Barzilai-Borwein steplengths

Stefania Bellavia <sup>a</sup>, Benedetta Morini <sup>a,\*</sup>, Mahsa Yousefi <sup>a</sup>

<sup>a</sup>*Department of Industrial Engineering, University of Florence, Viale G.B Morgagni 40,  
Florence, 50134 (FI), Italy*

---

## Abstract

We investigate on stochastic gradient methods and stochastic counterparts of the Barzilai-Borwein steplengths and their application to finite-sum minimization problems. Our proposal is based on the Trust-Region-ish (TRish) framework introduced in [F. E. Curtis, K. Scheinberg, R. Shi, *A stochastic trust region algorithm based on careful step normalization*, *Informations Journal on Optimization*, 1, 2019]. The new framework, named TRishBB, aims at enhancing the performance of TRish and at reducing the computational cost of the second-order TRish variant. We propose three different methods belonging to the TRishBB framework and present the convergence analysis for possibly nonconvex objective functions, considering biased and unbiased gradient approximations. Our analysis requires neither diminishing step-sizes nor full gradient evaluation. The numerical experiments in machine learning applications demonstrate the effectiveness of applying the Barzilai-Borwein steplength with stochastic gradients and show improved testing accuracy compared to the TRish method.

*Keywords:* finite-sum minimization, stochastic trust-region methods, Barzilai-Borwein method, machine learning.

*2010 MSC:* 65K05, 90C30

---

\*Corresponding author

*Email addresses:* stefania.bellavia@unifi.it (Stefania Bellavia )  
benedetta.morini@unifi.it (Benedetta Morini )  
mahsa.yousefi@unifi.it (Mahsa Yousefi )

## 1. Introduction

We consider the following optimization problem

$$\min_{x \in \mathbb{R}^n} f(x) = \frac{1}{N} \sum_{i=1}^N f_i(x), \quad (1)$$

which minimizes a finite-sum function  $f$  with large  $N$ . We assume that each function  $f_i : \mathbb{R}^n \rightarrow \mathbb{R}$ ,  $i \in \mathcal{N} \stackrel{\text{def}}{=} \{1, \dots, N\}$ , is continuously differentiable. Several important problems can be stated in this form, e.g., classification problems in Machine Learning (ML) or Deep Learning (DL), data fitting problems, and sample average approximations of an objective function given in the form of mathematical expectation. In the class of first-order optimization methods, Gradient Descent (GD) methods generate iterations of the form

$$x_{k+1} = x_k - \mu_k \nabla f(x_k), \quad (2)$$

for some positive scalar  $\mu_k$  and  $k \geq 0$ . Convergence and efficiency of the GD method and more generally of gradient-based methods depend heavily on the sequence of the steplengths [1–3]. In [1] Barzilai and Borwein proposed to use a parameter  $\mu_k$  which attempts to capture second-order information without computing the Hessian matrix of  $f$  nor its inverse. In other words, the Barzilai-Borwein (BB) method can be regarded as a quasi-Newton method where the Hessian is approximated by  $\mu_k^{-1}I$ ,  $I \in \mathbb{R}^{n \times n}$  being the identity matrix, and  $\mu_k$  minimizes the least-squares error of a secant equation involving the difference between two successive iterates and the difference between two successive gradients.

Computing the gradient  $\nabla f(x_k)$  to perform the update (2) is practically inconvenient in ML and DL applications where  $f$  represents a loss function on a given dataset and  $N$  is large. The Stochastic Gradient (SG) method [4, 5] and the mini-batch SG method [6] are iterative procedures where the full gradient  $\nabla f(x_k)$  is replaced by either a single gradient  $\nabla f_i(x_k)$ ,  $i \in \mathcal{N}$  chosen randomly, or by a mini-batch of samples of the form  $\nabla f_{\mathcal{N}_k}(x_k) = \frac{1}{|\mathcal{N}_k|} \sum_{i \in \mathcal{N}_k} \nabla f_i(x_k)$  where the set  $\mathcal{N}_k \subseteq \mathcal{N}$  is chosen randomly and  $|\mathcal{N}_k|$  denotes its cardinality, i.e., the mini-batch size. A limitation of such methods is the need to choose problem-dependent steplengths to guarantee convergence. An attempt to reduce such dependence was made in [7] where the steplengths depend on a Trust-Region-ish (TRish) rule and normalized steps are selected whenever the norm of the stochastic gradient is within a prefixed

interval whose endpoints need to be tuned. TRish method was designed for both first-order models [7, 8] and quadratic models [9] and, contrary to a standard trust-region approach, does not test for actual versus predicted reduction and thus does not call for  $f$ -evaluations. Results from [7, 8] show that TRish can outperform a standard stochastic gradient approach and it was very recently extended to equality-constrained problems [10].

The aim of this work is to combine the TRish methodology and stochastic BB steplengths in order to employ second-order information at a low computational cost; the selection of BB steplengths is ruled by TRish automatically. We devise the computation of BB steplengths in a stochastic setting and provide a theoretical analysis without requiring either diminishing steplengths nor unbiased stochastic gradients. In addition, we design three different procedures belonging to the above framework and show numerical results where our procedures enhance the performance of the first-order TRish method [9].

This paper is organized as follows. The remainder of this section is devoted to a review of the relevant literature providing background, motivation, and contribution to our work. We outline the proposed stochastic algorithms in Section 2 and present the theoretical analysis in Section 3. In Section 4 we present the implementation details, experimental setup, and an extensive evaluation of the method’s performance. Finally, in Section 5 we provide an overview of the obtained results and perspectives.

**Notations.** The Euclidean norm is denoted as  $\|\cdot\|$ .  $\nabla f_{\mathcal{N}_k}(x_k)$  represents a stochastic gradient at iteration  $k$ , evaluated by sampling over a subset of indices  $\mathcal{N}_k \subseteq \mathcal{N}$  and it holds  $\nabla f_{\mathcal{N}_k}(x_k) = \frac{1}{|\mathcal{N}_k|} \sum_{i \in \mathcal{N}_k} \nabla f_i(x_k)$ ; an analogous notation is used for sampled Hessian approximations. We use the symbol  $|\cdot|$  to denote the absolute value of a scalar, the cardinality of a set and the number of columns of a matrix, the meaning will be clear from the context. The operation  $\lfloor \cdot \rfloor$  gives the nearest integer less than or equal to the operand. The modulo operation  $\mathbf{mod}(p, t)$  returns the remainder after division of  $p$  by  $t$ .  $\mathbb{E}_k[\cdot]$  and  $\mathbb{P}_k[\cdot]$  denote, respectively, the conditional expectation and probability given that the algorithm has reached  $x_k$  at the  $k$ -th iteration.

### 1.1. Related works and motivations

The use of BB steplengths combined with stochastic gradients calls for the definition of the stochastic counterparts of the standard BB steplengths and for convergence analysis in expectation or high probability of the resulting

procedures. Several attempts have been made [11–15] and typically originate from the class of stochastic quasi-Newton methods [16–22].

In [11], BB steplengths were incorporated into the Stochastic Variance Reduction Gradient (SVRG) method [23] and into the SG method. The proposed methods are inner-outer loop-based frameworks. Since SVRG provides a full gradient at each outer loop, the BB steplength was computed at outer loops using the standard formula for the BB steplength; convergence of the resulting procedure was proved for strongly convex objective functions. On the other hand, single stochastic gradients  $\nabla f_i$  were employed at each iteration in the SG method and, in the inner loop, a moving averaging rule over  $N$  stochastic gradients at different points was computed; then, such average was used at each outer loop to evaluate a stochastic BB parameter. A theoretical support for this method was not provided. In [12], deterministic BB steplengths from [24], based on exact gradient and function evaluations, were used in the SVRG method; convergence was analyzed for strongly convex objective functions. In [13], stochastic BB steplengths were formed by a moving averaging rule on mini-batch gradients evaluated at different points and selected if they lied within an interval with endpoints tending to zero. Using diminishing stepsizes provides convergence due to well-known results for SG method but, in principle, BB steplengths may be discarded eventually since they are not supposed to tend to zero. A further method in which stochastic BB steplengths were formed and diminishing stepsizes were imposed is given in [14]; the distinguish feature is that the mini-batch of sample is taken constant for a prefixed number of iterations with the aim to explore the underlying approximate Hessian spectrum. Finally, the paper [15] investigates on the use of BB steplengths combined with projected stochastic gradients for constrained optimization problems and with the objective function in the form of mathematical expectation.

The above mentioned papers show limitations such as use of diminishing stepsizes, use of increasing batch sizes  $|\mathcal{N}_k|$ , use of full gradient information, need for  $f$ -evaluations. Most of the theoretical results hold for convex or strongly convex objective functions. Our proposal overcomes the above drawbacks employing the TRish paradigm given in [7, 9] which allows to use a simple stochastic quadratic model inspired by the BB method and to select adaptively the step by a trust-region methodology not invoking  $f$ -evaluations. The algorithms proposed in this work are cheap to implement and supported by theoretical results for possibly nonconvex objective functions and for biased or unbiased gradients.

---

**Algorithm 1: TRishBB**

---

- 1: Choose an initial iterate  $x_0 \in \mathbb{R}^n$  and a parameter  $\mu_0 > 0$ .
- 2: Choose  $(\alpha, \gamma_1, \gamma_2)$  such that  $\alpha > 0$ ,  $0 < \gamma_2 \leq \gamma_1 < \infty$ .
- 3: **for**  $k = 0, 1, \dots$  **do**
- 4:   Set  $H_k = \mu_k^{-1}I$ .
- 5:   Compute a stochastic gradient  $g_k$ .
- 6:   Compute the solution  $p_k$  of the trust-region subproblem

$$\min_{p \in \mathbb{R}^n} m_k(p) = g_k^T p + \frac{1}{2} p^T H_k p \quad \text{s.t.} \quad \|p\| \leq \Delta_k, \quad (3)$$

where

$$\Delta_k = \begin{cases} \alpha \gamma_1 \|g_k\| & \text{if } \|g_k\| \in \left[0, \frac{1}{\gamma_1}\right) \\ \alpha & \text{if } \|g_k\| \in \left[\frac{1}{\gamma_1}, \frac{1}{\gamma_2}\right] \\ \alpha \gamma_2 \|g_k\| & \text{if } \|g_k\| \in \left(\frac{1}{\gamma_2}, \infty\right) \end{cases}. \quad (4)$$

- 7:   Set  $x_{k+1} = x_k + p_k$ .
  - 8:   Form a parameter  $\mu_{k+1} > 0$ .
  - 9: **end for**
- 

## 2. New Stochastic Trust-Region-ish Algorithms

In this section we present our trust-region-ish algorithm employing stochastic BB steplengths. First, we provide a brief overview of the BB gradient method in the deterministic setting [1, 25–27], second we describe the main features of the method denoted as TRishBB, finally we present three algorithms belonging to the TRishBB frameworks.

At  $k$ th iteration, the standard BB method employs the second-order model  $m_k(p) = \nabla f(x_k)^T p + \frac{1}{2} p^T H_k p$  where  $H_k = \mu_k^{-1}I$ ; thus the iterates have the form (2). Regarding the computation of the steplength, given  $x_{k+1}$ , the main idea of the BB method is to form the parameter  $\mu_{k+1}^{\text{BB}}$  which solves

$$\mu_{k+1}^{\text{BB}} = \operatorname{argmin}_{\mu} \|\mu^{-1} s_k - y_k\|^2 = \frac{s_k^T s_k}{s_k^T y_k}, \quad (5)$$

with  $s_k = x_{k+1} - x_k$ , and  $y_k = \nabla f(x_{k+1}) - \nabla f(x_k)$  commonly denoted as correction pair. If  $f$  is strictly convex, then the scalar  $\mu_{k+1}^{\text{BB}}$  is positive.

If  $f$  is twice continuously differentiable then  $\mu_{k+1}^{\text{BB}}$  is related to the spectrum of the Hessian matrix of  $f$  as follows. Given a symmetric matrix  $A \in \mathbb{R}^{n \times n}$ , let  $q(A, v)$  be the Rayleigh quotient associated to the vector  $v \in \mathbb{R}^n$ ; in addition, let  $\lambda_{\min}(A)$  and  $\lambda_{\max}(A)$  denote the smallest and largest eigenvalue of  $A$ , respectively. Then, by the mean value theorem [28, Th. 3.1.3], we have

$$\mu_{k+1}^{\text{BB}} = \frac{s_k^T s_k}{s_k^T \left( \int_0^1 \nabla^2 f(x_k + ts_k) dt \right) s_k} = \frac{1}{q \left( \int_0^1 \nabla^2 f(x_k + ts_k) dt, s_k \right)} \quad (6)$$

Thus,  $\mu_{k+1}^{\text{BB}} \in \left[ \frac{1}{\lambda_{\max} \left( \int_0^1 \nabla^2 f(x_k + ts_k) dt \right)}, \frac{1}{\lambda_{\min} \left( \int_0^1 \nabla^2 f(x_k + ts_k) dt \right)} \right]$  if  $f$  is strictly convex. On the other hand, for a general function  $f$ ,  $\mu_{k+1}^{\text{BB}}$  is related to the spectrum of the matrix  $\int_0^1 \nabla^2 f(x_k + ts_k) dt$  by means of (6) but it may be negative.

In the BB method,  $H_{k+1} = \mu_{k+1}^{-1} I$  is formed using  $|\mu_{k+1}^{\text{BB}}|$  and thresholding  $|\mu_{k+1}^{\text{BB}}|$  by means of two prefixed scalars  $0 < \mu_{\min} < \mu_{\max}$ , i.e., setting  $\mu_{k+1} = \max\{\mu_{\min}, \min\{|\mu_{k+1}^{\text{BB}}|, \mu_{\max}\}\}$  to prevent excessively small or large values; in the case of convex problems it trivially holds  $\mu_{k+1} = \max\{\mu_{\min}, \min\{\mu_{k+1}^{\text{BB}}, \mu_{\max}\}\}$ . We refer to [27] for a survey on both practical rules for fixing  $\mu_{k+1}$  and step acceptance rules in the deterministic convex and nonconvex settings.

Now we analyze Algorithm 1 which is based on the second-order version of TRish in [9] and specialized to the case where the Hessian matrix is approximated by the diagonal matrix  $H_k = \mu_k^{-1} I, \forall k$ . Our goal is to use steplengths  $\mu_k$ 's inspired by the BB method and to enhance the first-order version of TRish [7] where  $H_k = 0$  for all  $k \geq 0$ . However, since stochastic gradients are available, the correction pair  $(s_k, y_k)$  is not uniquely defined and  $\mu_{k+1}^{\text{BB}}$  in (5) is a random parameter. The choice of the pair  $(s_k, y_k)$  is crucial for the practical behaviour of the method and we postpone the discussion of three options for the definition of  $(s_k, y_k)$  and  $\mu_{k+1}$  to Subsections 2.1-2.3.

At the generic  $k$ -th iteration of TRishBB, the stochastic gradient  $g_k$  is computed. Then, given the trust-region radius  $\Delta_k$  and the scalar  $\mu_k > 0$ , we set  $H_k = \mu_k^{-1} I$  and let (3) be the trust-region problem with strictly convex quadratic model. The trust-region solution is cheap to compute and takes the form

$$p_k = \begin{cases} -\mu_k g_k & \text{if } \|\mu_k g_k\| < \Delta_k, \\ -\frac{\Delta_k}{\|g_k\|} g_k & \text{otherwise.} \end{cases} \quad (7)$$

When  $p_k$  takes the form  $p_k = -H_k^{-1}g_k = -\mu_k g_k$ , it holds  $\|p_k\| < \Delta_k$  and  $p_k$  is the unconstrained minimizer of the model  $m_k$ . We refer to such a step as the unconstrained solution of (3). Otherwise, the solution lies on the boundary of the trust-region and it is the constrained Cauchy point; we will refer to this step as the constrained solution. In both cases,  $p_k$  is a step along  $(-g_k)$  and the cost for solving the trust-region problem is low. On the contrary, using a second-order trust-region methods and a general  $H_k$  requires a linear algebra phase such as the application of the conjugate gradient method [28, §7.5.1].

The updating rule (4) for  $\Delta_k$  is a distinctive feature of TRish. It is ruled by three positive and prefixed scalars,  $\alpha$ ,  $\gamma_1$  and  $\gamma_2$  and the magnitude of the norm of  $g_k$ . The insight of this rule is given in [7, §2]; briefly, adopting the standard rule, i.e., setting  $\Delta_k = \alpha$ , and thus normalizing  $(-g_k)$  if the trust-region solution is constrained, may cause the algorithm to compute ascent directions more likely than descent directions and then fail to progress in expectation. We note that in [7, 9] the algorithm admits the use of positive sequences  $\{\alpha_k\}$ ,  $\{\gamma_{1,k}\}$  and  $\{\gamma_{2,k}\}$  but here we focus on the choice of constant parameters.

Due to (4) and (7), the constrained trust-region solution has the form

$$p_k = \begin{cases} -\alpha\gamma_1 g_k & \text{if } \|g_k\| \in \left[0, \frac{1}{\gamma_1}\right), \\ -\alpha \frac{g_k}{\|g_k\|} & \text{if } \|g_k\| \in \left[\frac{1}{\gamma_1}, \frac{1}{\gamma_2}\right], \\ -\alpha\gamma_2 g_k & \text{if } \|g_k\| \in \left(\frac{1}{\gamma_2}, \infty\right), \end{cases} \quad (8)$$

analogously to the first-order TRish method in [7], whereas the unconstrained trust-region solution is  $p_k = -\mu_k g_k$  when

$$\mu_k < \begin{cases} \alpha\gamma_1 & \text{if } \|g_k\| \in \left[0, \frac{1}{\gamma_1}\right), \\ \frac{\alpha}{\|g_k\|} & \text{if } \|g_k\| \in \left[\frac{1}{\gamma_1}, \frac{1}{\gamma_2}\right], \\ \alpha\gamma_2 & \text{if } \|g_k\| \in \left(\frac{1}{\gamma_2}, \infty\right). \end{cases} \quad (9)$$

Importantly, once the step  $p_k$  is formed, the new iterate  $x_{k+1}$  is computed without performing the standard test of trust-region methods on predicted versus actual reduction [28]; thus the Algorithm TRishBB does not require the evaluation of the objective function  $f$ .

---

**Algorithm 2: TRishBB\_v1 (Iteration  $k$ )**

---

- 1: Given  $x_k \in \mathbb{R}^n$ ,  $(\alpha, \gamma_1, \gamma_2)$ ,  $\mu_k > 0$ ,  $0 < \mu_{min} < \mu_{max}$ ,  $m \geq 1$ .
  - 2: Choose  $\mathcal{N}_k \subseteq \mathcal{N}$ , compute  $g_k = \nabla f_{\mathcal{N}_k}(x_k)$  and set  $H_k = \mu_k^{-1}I$ .
  - 3: Obtain  $p_k$  from (7) and set  $x_{k+1} = x_k + p_k$ .
  - 4: **if**  $\text{mod}(k, m) = 0$  **then**
  - 5:    $s_k = p_k$  and  $y_k = \nabla f_{\mathcal{N}_k}(x_{k+1}) - g_k$
  - 6:    $\mu_{k+1} = \max \left\{ \mu_{min}, \min \left\{ \left| \frac{s_k^T s_k}{s_k^T y_k} \right|, \mu_{max} \right\} \right\}$
  - 7: **else**
  - 8:    $\mu_{k+1} = \mu_k$
  - 9: **end if**
- 

We conclude this section noting that each step  $p_k$  taken by TRishBB is along  $(-g_k)$  as in a first-order method but the unconstrained trust-region solution aims to exploit some second-order information via  $\mu_k$ .

In the following subsections we explore three ways to form stochastic BB steplengths; each of them provides a variant of the general Algorithm TRishBB.

### 2.1. *TRishBB\_v1*

The displayed Algorithm TRishBB\_v1 is a straightforward implementation of the BB method employing stochastic gradients and guidelines from stochastic quasi-Newton methods. Specifically, once the trust-region solution  $p_k$  in (7) is computed, the successive steplength  $\mu_{k+1}$  is formed using the correction pair  $(s_k, y_k)$  at line 5 of this algorithm. The vector  $s_k$  coincides with  $p_k$ , i.e., it is the step between  $x_{k+1}$  and  $x_k$  whereas the vector  $y_k$  is the difference between the mini-batch gradients  $\nabla f_{\mathcal{N}_k}(x_{k+1})$  and  $\nabla f_{\mathcal{N}_k}(x_k)$ . We underline that using the same set of indices  $\mathcal{N}_k$  in the computation of  $y_k$  is suggested in [29, 16, 17] and implies that (6) holds with the matrix  $\int_0^1 \nabla^2 f_{\mathcal{N}_k}(x_k + ts_k)$ . Thus, the BB steplength inherits spectral information as long as it is positive and  $f$  is twice continuously differentiable. Following a heuristic common rule, see e.g., [30], given an integer  $m \geq 1$ , the parameter  $\mu_{k+1}$  is updated every  $m$  iterations.

### 2.2. *TRishBB\_v2*

In Algorithm TRishBB\_v1 the pair  $(s_k, y_k)$  contains information from one single iteration and  $y_k$  is obtained using stochastic gradients, possibly

---

**Algorithm 3: TRishBB\_v2** (Iteration  $k$ )

---

- 1: Given  $x_k \in \mathbb{R}^n$ ,  $(\alpha, \gamma_1, \gamma_2)$ ,  $\mu_k > 0$ ,  $0 < \mu_{min} < \mu_{max}$ ,  $m \geq 1$ ,  $\beta = \frac{m-1}{m}$ ,  $\eta \in (0, 1)$ ,  $\bar{x}_{old}$ ,  $\bar{g}_{old}$ , and  $\bar{g}$  (if  $k = 0$ , then  $\bar{x}_{old} = x_0$ ,  $\bar{g}_{old} = 0$ ,  $\bar{g} = 0$ , and  $\bar{\mu}_0 = \mu_0$ ):
  - 2: Choose  $\mathcal{N}_k \subseteq \mathcal{N}$ , compute  $g_k = \nabla f_{\mathcal{N}_k}(x_k)$  and set  $H_k = \mu_k^{-1}I$ ;
  - 3: Obtain  $p_k$  from (7) and set  $x_{k+1} = x_k + p_k$ ;
  - 4: Compute  $\bar{g} = \beta\bar{g} + (1 - \beta)g_k$ ;
  - 5: **if**  $k > 0$  and **mod**( $k, m$ ) = 0 **then**
  - 6:    $\bar{x} = x_{k+1}$ ;
  - 7:    $s_k = \bar{x} - \bar{x}_{old}$  and  $y_k = \bar{g} - \bar{g}_{old}$ ;
  - 8:    $\hat{\mu}_k = \frac{1}{m} \begin{vmatrix} s_k^T s_k \\ s_k^T y_k \end{vmatrix}$ ,  $\bar{\mu}_{k+1} = \eta\bar{\mu}_k + (1 - \eta)\hat{\mu}_k$ ;
  - 9:    $\mu_{k+1} = \max\{\mu_{min}, \min\{\bar{\mu}_{k+1}, \mu_{max}\}\}$ ;
  - 10:    $\bar{x}_{old} = \bar{x}$ ,  $\bar{g}_{old} = \bar{g}$ , and  $\bar{g} = 0$ ;
  - 11: **else**
  - 12:    $\mu_{k+1} = \mu_k$ ;
  - 13: **end if**
- 

evaluated on a small sample  $\mathcal{N}_k$ . On the contrary, Algorithm TRishBB\_v2 forms a correction pair that accumulates information over a prefixed number  $m$  of iterations and is described below.

The vector  $s_k$  is the difference between two, not consecutive, iterates; the indices of such iterates differ by  $m$ , see lines 7 and 10 of the algorithm. The vector  $y_k$  is the difference between vectors computed via a moving average rule which accumulates stochastic gradients over  $m$  iterations, see lines 4, 7 and 10 of the algorithm; in particular  $\bar{g}$  is formed over the last  $m$  iterations while  $\bar{g}_{old}$  is the analogous vector formed in the previous cycle of  $m$  iterations. The parameter  $\beta = (m-1)/m$  is fixed in accordance with [31] to avoid hyperparameter tuning.

The form of  $s_k$  and  $y_k$  is borrowed from the BB-SGD algorithm [11] where  $|\mathcal{N}_k| = 1$ ,  $\forall k$ , and  $m = N$ , i.e.,  $N$  single gradient evaluations are performed before updating the steplength. In TRishBB\_v2 we allow  $|\mathcal{N}_k| > 1$ ; letting  $N_b = \lfloor N/|\mathcal{N}_k| \rfloor$  be (roughly) the number of disjoint mini-batches of size  $|\mathcal{N}_k|$  in  $\mathcal{N}$  and  $m = N_b$ , the cost for computing  $\bar{g}$  every  $m$  iterations is (roughly) the cost for one full gradient evaluation.

The steplength  $\mu_{k+1}$  is updated every  $m$  iterations and computed using accumulated information, see lines 8 and 9 of the algorithm. Given  $\eta \in$

---

**Algorithm 4: TRishBB\_v3** (Iteration  $k$ )

---

- 1: Given  $x_k \in \mathbb{R}^n$ ,  $(\alpha, \gamma_1, \gamma_2)$ ,  $\mu_k > 0$  with  $0 < \mu_{min} < \mu_{max}$ ,  $m \geq 1$ ,  $L \in \mathbb{N}$   
 $F_k \in \mathbb{R}^{n \times d}$  with  $d \leq L$ ,  $x_{avg}$ , and  $\bar{x}_{old}$ , (if  $k = 0$ , then  $F_0 = []$ ,  $x_{avg} = 0$ , and  $\bar{x}_{old} = 0$ ).
  - 2:  $x_{avg} = x_{avg} + x_k$
  - 3: Choose  $\mathcal{N}_k \subseteq \mathcal{N}$ , compute  $g_k = \nabla f_{\mathcal{N}_k}(x_k)$  and set  $H_k = \mu_k^{-1}I$ .
  - 4: Obtain  $p_k$  from (7) and set  $x_{k+1} = x_k + p_k$ .
  - 5: **if**  $k \leq L$  **then**
  - 6:   Store  $g_k$  in  $k$ th column of  $F_k$ .
  - 7: **else**
  - 8:   Remove the first column of  $F_k$ , and store  $g_k$  in its  $L$ -th column.
  - 9: **end if**
  - 10: **if**  $\text{mod}(k, m) = 0$  **then**
  - 11:    $\bar{x} = \frac{x_{avg}}{m}$ , and  $x_{avg} = 0$
  - 12:   **if**  $k > 0$  **then**
  - 13:      $s_k = \bar{x} - \bar{x}_{old}$ , and  $y_k = \frac{1}{|F_k|} F_k (F_k^T s_k)$
  - 14:      $\mu_{k+1} = \max \left\{ \mu_{min}, \min \left\{ \left| \frac{s_k^T s_k}{s_k^T y_k} \right|, \mu_{max} \right\} \right\}$
  - 15:   **end if**
  - 16:    $\bar{x}_{old} = \bar{x}$
  - 17: **else**
  - 18:    $\mu_{k+1} = \mu_k$
  - 19: **end if**
- 

$(0, 1)$ , the scalar  $\bar{\mu}_{k+1}$  is computed as the convex combination of the current stochastic BB steplength  $\hat{\mu}_k$  and the current accumulated parameter  $\bar{\mu}_k$ . The larger  $\eta$  is, the higher the penalization to  $\hat{\mu}_k$  is and this may soften the effect of intrinsic noise arising from stochastic gradients.

### 2.3. TRishBB\_v3

Algorithm TRishBB\_v3 is originated by the arguments in [32] to avoid both the potentially harmful effects of the gradient difference when  $\|s_k\|$  is small and the noise in stochastic gradient estimates. In [32], given  $s_k = \bar{x} - \bar{x}_{old}$  for some  $\bar{x}$ ,  $\bar{x}_{old}$ , the vector  $y_k$  is defined as  $y_k = \nabla^2 f_{\widetilde{\mathcal{N}}_k}(\bar{x}) s_k$  where  $\nabla^2 f_{\widetilde{\mathcal{N}}_k}(\bar{x})$  is a subsampled Hessian approximation and  $|\widetilde{\mathcal{N}}_k|$  is supposed to be larger than the batch size used for gradients. If the objective function  $f$  is the cross-entropy loss function or the least-squares function, then  $\nabla^2 f_{\widetilde{\mathcal{N}}_k}(\bar{x})$  can be approximated by the empirical Fisher Information Matrix (FIM) [33,

§11] defined as

$$\frac{1}{|\mathcal{N}_k|} \sum_{i \in \mathcal{N}_k} \nabla f_i(\bar{x}) \nabla f_i(\bar{x})^T.$$

Empirical FIM has a higher per-iteration cost than first-order methods, thus it was further simplified by introducing the *accumulated* empirical FIM [34, 35].

In Algorithm TRishBB\_v3, we update  $s_k$  and  $y_k$  every  $m$  iterations and  $y_k$  is computed as the accumulated empirical FIM. In particular, as displayed in line 13 of the algorithm,  $s_k$  is formed using the averages  $\bar{x}$  and  $\bar{x}_{old}$ ;  $\bar{x}$  is the average of the last  $m$  iterates, and  $\bar{x}_{old}$  is the average of the previous  $m$  iterates, see lines 2 and 11 of the algorithm. Average iterates are meant to represent more stable approximations than a single iterate for computing the difference  $s_k$ . Concerning  $y_k$ , let  $F_k$  be the limited memory matrix whose columns contain the last  $L$  computed stochastic gradients for some positive integer  $L$ . Then, the curvature vector  $y_k$  is defined as  $y_k = \frac{1}{|F_k|} F_k (F_k^T s_k)$ , see line 13 of the algorithm, where  $|F_k|$  denotes the number of columns of  $F_k$ . Since  $F_k F_k^T$  is the sum of  $|F_k|$  rank-one matrices, (6) implies

$$\mu_{k+1}^{\text{BB}} = \frac{1}{\frac{1}{|F_k|} \sum_{t=k-|F_k|+1}^k q(\nabla f_{\mathcal{N}_t}(x_t)(\nabla f_{\mathcal{N}_t}(x_t))^T, s_k)},$$

where  $\nabla f_{\mathcal{N}_t}(x_t)(\nabla f_{\mathcal{N}_t}(x_t))^T$  is a rank-one matrix.

### 3. Convergence Analysis

We present the convergence analysis of TRishBB considering the use of both biased and unbiased stochastic gradients. Further, we investigate the case where the function  $f$  satisfies the Polyak-Lojasiewicz (PL) condition and the case where  $f$  is a general nonconvex function.

The assumption of the objective function made in our analysis and the PL condition are presented below.

**Assumption 3.1.** *Function  $f : \mathbb{R}^n \rightarrow \mathbb{R}$  is continuously differentiable, bounded below by  $f_*$ , and there exists a positive  $L$  such that*

$$f(x) \leq f(y) + \nabla f(y)^T(x - y) + \frac{L}{2} \|x - y\|^2 \quad \text{for all } x, y \in \mathbb{R}^n. \quad (10)$$

**Assumption 3.2.** For any  $x \in \mathbb{R}^n$ , the Polyak-Lojasiewicz (PL) condition holds with  $c \in (0, \infty)$ , i.e.,

$$2c(f(x) - f_*) \leq \|\nabla f(x)\|^2 \text{ for all } x \in \mathbb{R}^n. \quad (11)$$

In our analysis we characterize the iterations of TRishBB by three cases: “Case 1”:  $\|g_k\| \in [0, \frac{1}{\gamma_1})$ , “Case 2”:  $\|g_k\| \in [\frac{1}{\gamma_1}, \frac{1}{\gamma_2}]$ , and “Case 3”:  $\|g_k\| \in (\frac{1}{\gamma_2}, \infty)$ . We denote by  $C_{i,k}$  the events where Case  $i$  occurs, for  $i \in \{1, 2, 3\}$ .

### 3.1. Analysis with Biased Gradients

The results presented in this subsection concern biased gradients satisfying the following assumption.

**Assumption 3.3.** There exist positive  $\omega, M_1, M_2$  such that the stochastic gradient  $g_k$  satisfy

$$\nabla f(x_k)^T \mathbb{E}_k[g_k] \geq \omega \|\nabla f(x_k)\|^2, \quad (12)$$

$$\mathbb{E}_k[\|g_k\|^2] \leq M_1 + M_2 \|\nabla f(x_k)\|^2. \quad (13)$$

The inequality (13) implies that

$$\mathbb{P}_k[\mathcal{E}_k] \mathbb{E}_k[\nabla f(x_k)^T g_k | \mathcal{E}_k] \leq h_1 + h_2 \|\nabla f(x_k)\|^2, \quad (14)$$

with  $h_1 = \frac{1}{2}\sqrt{M_1}$  and  $h_2 = h_1 + \sqrt{M_2}$ ; see [7, Lemma 2].

We also make the following assumption of the parameter  $\mu_{min}$ .

**Assumption 3.4.** Given positive  $\mu_{min}$ , for all  $k \geq 0$ , it holds

$$\mu_{min} \leq \gamma_2 \alpha.$$

The results presented are based on the analysis developed by [7]. The following two lemma are technical results. As for the notation, for the events of taking the unconstrained and the constrained solutions (7) we use the notations  $S_{BB}$  and  $\overline{S_{BB}}$ , respectively. Moreover, for the events  $C_{i,k}$ ,  $i \in \{1, 2, 3\}$ , that occur within each defined case we set  $C_{i,k}^{BB} \stackrel{\text{def}}{=} C_{i,k} \cap S_{BB}$  and  $\overline{C_{i,k}^{BB}} \stackrel{\text{def}}{=} C_{i,k} \cap \overline{S_{BB}}$ . Finally, we denote with  $\mathcal{E}_k$  the event that  $\nabla f(x_k)^T g_k \geq 0$  and with  $\overline{\mathcal{E}_k}$  the event that  $\nabla f(x_k)^T g_k < 0$ .

**Lemma 3.1.** *Under Assumptions 3.1 and 3.4, the iterates generated by Algorithm TRishBB satisfy*

$$\begin{aligned} \mathbb{E}_k[f(x_{k+1})] - f(x_k) &\leq (\gamma_1\alpha - \mu_{min})\mathbb{P}_k[\mathcal{E}_k]\mathbb{E}_k[\nabla f(x_k)^T g_k | \mathcal{E}_k] \\ &\quad + \frac{L}{2}\gamma_1^2\alpha^2\mathbb{E}_k[\|g_k\|^2] - \gamma_1\alpha\mathbb{E}_k[\nabla f(x_k)^T g_k], \end{aligned} \quad (15)$$

for all  $k$ , where  $\mathcal{E}_k$  is the event that  $\nabla f(x_k)^T g_k \geq 0$ .

*Proof.* See Appendix B.1.  $\square$

**Lemma 3.2.** *Under Assumptions 3.1, 3.3, and 3.4, the iterates generated by Algorithm TRishBB satisfy*

$$\begin{aligned} \mathbb{E}_k[f(x_{k+1})] - f(x_k) &\leq (\gamma_1\alpha - \mu_{min})h_1 + \frac{L}{2}\gamma_1^2\alpha^2M_1 \\ &\quad - \gamma_1\alpha\left(\omega - \frac{L}{2}\gamma_1M_2\alpha\right)\|\nabla f(x_k)\|^2 + (\gamma_1\alpha - \mu_{min})h_2\|\nabla f(x_k)\|^2, \end{aligned} \quad (16)$$

for all  $k$  with  $h_1, h_2$  given in (14).

*Proof.* It is a direct consequence of Assumption 3.3, Lemma 3.1 and (14).  $\square$

For the rest of analysis, we define

$$\theta_1 = \frac{1}{2}\omega\gamma_1 - h_2(\gamma_1 - \rho\gamma_2), \quad \theta_2 = h_1(\gamma_1\alpha - \mu_{min}) + \frac{1}{2}\gamma_1^2LM_1\alpha^2, \quad (17)$$

where  $\rho = \frac{\mu_{min}}{\alpha\gamma_2} \in (0, 1]$ ,  $h_1$  and  $h_2$  are given in (14),  $\omega$  and  $M_1$  are given in Assumption 3.3. Note that  $\theta_1$  is positive for any choice of  $(\gamma_1, \gamma_2)$  in the case  $h_2 - \frac{1}{2}\omega \leq 0$ , while condition

$$\frac{\gamma_1}{\gamma_2} < \frac{\rho h_2}{h_2 - \frac{1}{2}\omega} \quad (18)$$

ensures  $\theta_1 > 0$  in the case  $h_2 - \frac{1}{2}\omega > 0$ . Further, note that  $\theta_2$  is positive by Assumption 3.4.

First we consider the case where the objective function satisfy the Polyak-Lojasiewicz condition (3.2), then we analyze the general case.

**Theorem 3.1.** Under Assumptions 3.1–3.4, suppose that (18) holds in case  $h_2 - \frac{1}{2}\omega > 0$  and that

$$\alpha \leq \min \left\{ \frac{\omega}{\gamma_1 LM_2}, \frac{1}{2c\theta_1} \right\}, \quad (19)$$

with  $h_2$  given in (14) and  $\theta_1$  given in (17). Then, the expected optimality gap of the iterates generated by Algorithm TRishBB satisfies

$$\mathbb{E}[f(x_{k+1})] - f_* \xrightarrow{k \rightarrow \infty} \frac{\theta_2}{2c\alpha\theta_1}, \quad (20)$$

where  $\theta_2$  is given in (17).

*Proof.* By (19) and (16), it follows that

$$\mathbb{E}_k[f(x_{k+1})] - f(x_k) \leq -\alpha\theta_1 \|\nabla f(x_k)\|^2 + \theta_2,$$

for all  $k$  and  $\theta_1, \theta_2$  defined in (17). Therefore, (11) implies that

$$\mathbb{E}_k[f(x_{k+1})] - f(x_k) \leq -2c\alpha\theta_1(f(x_k) - f_*) + \theta_2. \quad (21)$$

Adding and subtracting  $f_*$  on the left-hand side, taking total expectations, and rearranging give

$$\begin{aligned} \mathbb{E}[f(x_{k+1})] - f_* &\leq (1 - 2c\alpha\theta_1)(\mathbb{E}[f(x_k)] - f_*) + \theta_2 \\ &= \frac{\theta_2}{2c\alpha\theta_1} + (1 - 2c\alpha\theta_1)(\mathbb{E}[f(x_k)] - f_*) + \theta_2 - \frac{\theta_2}{2c\alpha\theta_1} \\ &= \frac{\theta_2}{2c\alpha\theta_1} + (1 - 2c\alpha\theta_1) \left( \mathbb{E}[f(x_k)] - f_* - \frac{\theta_2}{2c\alpha\theta_1} \right). \end{aligned} \quad (22)$$

Since  $1 - 2c\alpha\theta_1 \in (0, 1)$ , this represents a contraction inequality. Applying the result repeatedly through iteration  $k$ , one obtains the desired result.  $\square$

**Theorem 3.2.** Under Assumptions 3.1, 3.3 and 3.4, suppose that (18) holds in case  $h_2 - \frac{1}{2}\omega > 0$  and that

$$\alpha \leq \frac{\omega}{\gamma_1 LM_2}, \quad (23)$$

with  $h_2$  given in (14) and  $\theta_1$  given in (17). Then the iterates generated by Algorithm TRishBB satisfy

$$\sum_{k=0}^K \mathbb{E} \left[ \frac{1}{K} \|\nabla f(x_k)\|^2 \right] \xrightarrow{K \rightarrow \infty} \frac{\theta_2}{\alpha\theta_1}, \quad (24)$$

where  $\theta_2$  is given in (17).

*Proof.* By (23) and (16), it follows that

$$\mathbb{E}_k[f(x_{k+1})] - f(x_k) \leq -\alpha\theta_1\|\nabla f(x_k)\|^2 + \theta_2,$$

for all  $k$  and  $\theta_1, \theta_2$  defined in (17). Therefore, taking total expectation yields

$$\mathbb{E}[\|\nabla f(x_k)\|^2] \leq \frac{1}{\alpha\theta_1} (\mathbb{E}[f(x_k)] - \mathbb{E}[f(x_{k+1})]) + \frac{\theta_2}{\alpha\theta_1}. \quad (25)$$

Summing both sides for  $k \in \{1, 2, \dots, K\}$  gives

$$\begin{aligned} \sum_{k=0}^K \mathbb{E}[\|\nabla f(x_k)\|^2] &\leq \frac{1}{\alpha\theta_1} (f(x_0) - \mathbb{E}[f(x_{K+1})]) + \frac{K\theta_2}{\alpha\theta_1} \\ &\leq \frac{f(x_0) - f_*}{\alpha\theta_1} + \frac{K\theta_2}{\alpha\theta_1}. \end{aligned}$$

Dividing by  $K$  concludes the proof.  $\square$

### 3.2. Analysis with Unbiased Gradients

In this subsection we assume that  $g_k$  is unbiased estimator of the true gradient with bounded variance. Such assumption is summarized below.

**Assumption 3.5.** *For all  $k$ ,  $g_k$  is an unbiased estimator of the gradient  $\nabla f(x_k)$ , i.e.,  $\mathbb{E}_k[g_k] = \nabla f(x_k)$ . For all  $k$ , there exist a positive constant  $M_g$  such that*

$$\mathbb{E}_k[\|\nabla f(x_k) - g_k\|^2] \leq M_g. \quad (26)$$

Since  $g_k$  is unbiased, it follows.

$$\begin{aligned} \mathbb{E}_k[\|\nabla f(x_k) - g_k\|^2] &= \mathbb{E}_k[\|\nabla f(x_k)\|^2 - 2\nabla f(x_k)^T g_k + \|g_k\|^2] \\ &= -\|\nabla f(x_k)\|^2 + \mathbb{E}_k[\|g_k\|^2]. \end{aligned} \quad (27)$$

Hence Assumption (3.3) is satisfied with  $\omega = 1$ ,  $M_1 = M_g$ ,  $M_2 = 1$  and the convergence results of §3.1 hold. Now we further characterize the convergence without imposing bounds, such as inequality (18), on  $\gamma_1, \gamma_2$ . The first lemma is a technical result.

**Lemma 3.3.** *Suppose that Assumption 3.1 holds and*

$$0 < \alpha \leq \frac{\gamma_2}{8\gamma_1^2 L}, \quad \mu_{\min} \geq \frac{4\gamma_1\alpha}{5}. \quad (28)$$

Then, the  $k$ -th iterate generated by Algorithm TRishBB satisfies

$$\mathbb{E}_k[f(x_{k+1})] - f(x_k) \leq -\frac{1}{16}\gamma_2\alpha\mathbb{E}_k[\|g_k\|^2] + \frac{\gamma_1^2}{\gamma_2}\alpha\mathbb{E}_k[\|\nabla f(x_k) - g_k\|^2], \quad (29)$$

$$\mathbb{E}_k[f(x_{k+1})] - f(x_k) \leq -\frac{1}{16}\gamma_2\alpha\|\nabla f(x_k)\|^2 + \alpha\left(\frac{\gamma_1^2}{\gamma_2} - \frac{1}{16}\gamma_2\right)M_g. \quad (30)$$

*Proof.* See Appendix B.2.  $\square$

In case the objective function satisfies the Polyak-Lojasiewicz condition (3.2), the expected optimality gap is bounded above by a sequence that converges linearly to a constant proportional to  $M_g/c$ .

**Theorem 3.3.** *Suppose that Assumptions 3.1, 3.2 and 3.5 hold and that*

$$0 < \alpha < \min\left\{\frac{\gamma_2}{8\gamma_1^2L}, \frac{8}{\gamma_2c}\right\}, \quad \mu_{\min} \geq \frac{4\gamma_1\alpha}{5}. \quad (31)$$

Then, the sequence generated by Algorithm TRishBB satisfies

$$\mathbb{E}[f(x_{k+1})] - f_* \xrightarrow{k \rightarrow \infty} \frac{8\theta_3M_g}{\gamma_2c}, \quad (32)$$

for all  $k$ , where  $\theta_3 = \left(\frac{\gamma_1^2}{\gamma_2} - \frac{\gamma_2}{16}\right)$ .

*Proof.* By (30) and (11) we obtain

$$\mathbb{E}_k[f(x_{k+1})] - f(x_k) \leq -\frac{1}{8}\gamma_2\alpha c(f(x_k) - f_*) + \alpha\theta_3M_g. \quad (33)$$

Taking total expectation, for all  $k$  we have

$$\begin{aligned} \mathbb{E}[f(x_{k+1})] - f_* &\leq \frac{8\theta_3M_g}{\gamma_2c} + \left(1 - \frac{1}{8}\gamma_2\alpha c\right) (\mathbb{E}[f(x_k)] - f_*) + \alpha\theta_3M_g - \frac{8\theta_3M_g}{\gamma_2c} \\ &= \frac{8\theta_3M_g}{\gamma_2c} + \left(1 - \frac{1}{8}\gamma_2\alpha c\right) \left(\mathbb{E}[f(x_k)] - f_* - \frac{8\theta_3M_g}{\gamma_2c}\right). \end{aligned} \quad (34)$$

Since  $(1 - \frac{1}{8}\gamma_2\alpha c) \in (0, 1)$ , this represents a contraction inequality. Applying the result repeatedly through iteration  $k$ , one obtains the desired result.  $\square$

When  $f$  is a nonconvex function, the expected average squared norm of the gradient converges to  $\left(\frac{16\gamma_1^2}{\gamma_2^2} - 1\right) M_g$ .

**Theorem 3.4.** *Suppose that Assumptions 3.1, 3.5 hold and that*

$$0 < \alpha \leq \frac{\gamma_2}{8\gamma_1^2 L}, \quad \mu_{min} \geq \frac{4\gamma_1\alpha}{5}. \quad (35)$$

*Then, the sequence generated by Algorithm TRishBB satisfies*

$$\mathbb{E} \left[ \frac{1}{K} \sum_{k=1}^K \|\nabla f(x_k)\|^2 \right] \xrightarrow{K \rightarrow \infty} \left( \frac{16\gamma_1^2}{\gamma_2^2} - 1 \right) M_g.$$

*Proof.* Consider (30). Taking total expectation, it follows for all  $k$  that

$$\mathbb{E}[f(x_{k+1})] - \mathbb{E}[f(x_k)] \leq -\frac{1}{16}\gamma_2\alpha\mathbb{E}[\|\nabla f(x_k)\|^2] + \alpha \left( \frac{\gamma_1^2}{\gamma_2} - \frac{1}{16}\gamma_2 \right) M_g, \quad (36)$$

which implies

$$\mathbb{E}[\|\nabla f(x_k)\|^2] \leq \frac{16}{\gamma_2\alpha} (\mathbb{E}[f(x_k)] - \mathbb{E}[f(x_{k+1})]) + \left( \frac{16\gamma_1^2}{\gamma_2^2} - 1 \right) M_g. \quad (37)$$

The proof is concluded by summing this inequality over all  $k \in \{1, \dots, K\}$  and using the fact that  $f$  is bounded below by  $f_*$ .  $\square$

## 4. Numerical Experiments

In this section, we present experimental results to compare Algorithms TRishBB\_v1, TRishBB\_v2 and TRishBB\_v3 with the first-order version of TRish in [7], i.e., Algorithm TRishBB with  $\mu_k = 0, \forall k$ . All experiments were conducted with MATLAB (R2024a) on a Rocky Linux 8.10 (64-bit) server with 256 GiB memory using an NVIDIA A100 PCIe GPU (with 80 GiB on-board memory).

### 4.1. Classification Problems

We consider some ML test problems of the form (1). Table 1 summarizes five test problems used in our experiments for both binary and multi-class classification tasks. Each test dataset with  $C$  possible classes is divided into training and testing sets, denoted as  $\{(a_i, b_i) \mid i \in \mathcal{N}\}$  and  $\{(a_i, b_i) \mid i \in \bar{\mathcal{N}}\}$ ,

Table 1: Classification test problems

Dataset	( $N, \bar{N}$ )	$d$	$n$	Type	$f_i(x)$	NN
<b>a1a</b> [36]	(1605, 29351)	123	123	Binary	Logistic regression	-
<b>w1a</b> [36]	(2477, 47272)	300	300	Binary	Logistic regression	-
<b>cina</b> [36]	(10000, 6033)	132	132	Binary	Logistic regression	-
<b>MNIST</b> [37]	(60000, 10000)	$28 \times 28 \times 1$	431030	Multi	Cross-entropy	NET-1
<b>CIFAR10</b> [38]	(50000, 10000)	$32 \times 32 \times 3$	545098	Multi	Cross-entropy	NET-2

with  $|\mathcal{N}| = N$  and  $|\bar{\mathcal{N}}| = \bar{N}$  samples, respectively; the values of  $N$  and  $\bar{N}$  are reported in the table. The vector  $a_i \in \mathbb{R}^d$  represents the  $i$ -th data with  $d$  features while  $b_i$  is the corresponding categorical label associated. The dataset **cina** was normalized such that each feature vector has components in the interval  $[0, 1]$ . For **MNIST** and **CIFAR10**, besides the zero-one rescaling, we implemented z-score normalization to have zero mean and unit variance. Precisely, all  $N$  training images, (3-D arrays of size  $h \times w \times c$  where  $h$ ,  $w$ , and  $c$  denote the height, width, and number of channels of the images, respectively), undergo normalization by subtracting the mean (a 3-D array) and dividing by the standard deviation (a 3-D array) component-wise. Data in the testing set are also normalized using the same statistics as in the training data.

For binary classification problems, we used logistic regression where the single loss function  $f_i(x)$  with  $x \in \mathbb{R}^n$  in (1) is defined as

$$f_i(x) = \log(1 + e^{-b_i(x^T a_i)}), \quad i = 1, \dots, N, \quad b_i \in \{+1, -1\}.$$

This model is used for the datasets **a1a**, **w1a**, and **cina**. Note that the number of unknown parameters in  $x \in \mathbb{R}^n$  is equal to the number of features in  $a_i \in \mathbb{R}^d$ , i.e.,  $n = d$ . For multi-classification problems, we used neural network models coupled with the softmax cross-entropy loss that is the single loss function  $f_i(x)$  with  $x \in \mathbb{R}^n$  in (1), and defined as

$$f_i(x) = - \sum_{k=1}^C (b_i)_k \log(h(a_i; x))_k, \quad i = 1, \dots, N.$$

We employ this model using the datasets **MNIST** and **CIFAR10** where  $a_i \in \mathbb{R}^d$  is a 3-D array (grayscale or RGB image), and the categorical label  $b_i$  is converted into a one-hot encoded vector; i.e., it is a binary vector of length  $C$ , where  $C - 1$  elements are zero except for the element whose index corresponds to the true class that is equal to one. The output  $h(a_i; \cdot)$  is a

Table 2: NN architecture

NET-1	<i>Input(d)</i> <i>Conv(5, 20, 1, 0)/ReLU/MaxPool(2 × 2, 2, 0)</i> <i>Conv(5, 50, 1, 0)/ReLU/MaxPool(2 × 2, 2, 0)</i> <i>FC(500)/ReLU</i> <i>FC(C)/Softmax</i>
NET-2	<i>Input(d)</i> <i>Conv(3, 32, 1, same)/ReLU/AveragePool(2 × 2, 2, 0)</i> <i>Conv(3, 64, 1, same)/ReLU/AveragePool(2 × 2, 2, 0)</i> <i>FC(128)/ReLU</i> <i>FC(C)/Softmax</i>

prediction provided by the neural network (NN) whose architecture is described in Table 2.<sup>1</sup> For MNIST dataset with grayscale images in  $C = 10$  classes (digits 0–9), and CIFAR10 with RGB images in  $C = 10$  categories (e.g., dogs and ships), we used NET-1 and NET-2 respectively. Note that the size  $n$  of problem (1) using an NN depends on both the number of features  $d$  and the depth of the network. We utilized the MATLAB Deep Learning Toolbox, leveraging automatic gradient computation in customized training loops; we used `forward` and `crossentropy` for implementing the NN softmax cross-entropy. See [39, Table2] for details on implementing NN classification problems by this toolbox.

#### 4.2. Experimental Configuration

Algorithm TRishBB\_v1 was run setting  $m = 20$  and selecting random and independent mini-batches  $\mathcal{N}_k$ , thus the gradients  $g_k$  are unbiased. Algorithm TRishBB\_v2 was run with  $\eta = 0.9$  and  $m = N_b = \lfloor N/|\mathcal{N}_k| \rfloor$  on the base of the discussion in §2.2; the mini-batches  $\mathcal{N}_k$  were selected as disjoint subsets of  $\mathcal{N}$  and the resulting gradients are biased. Algorithm TRishBB\_v3 was run setting  $m = 5$ ,  $L = 100$  as suggested in [34] and the mini-batch selection was as in TRishBB\_v1. For all  $k \geq 0$ , the mini-batch size for computing stochastic gradients in these variants was  $|\mathcal{N}_k| = 64$  for the datasets `a1a`, `w1a`, and `cina` and  $|\mathcal{N}_k| = 128$  for the datasets MNIST and CIFAR10. The values  $\mu_{\min}$ , and  $\mu_{\max}$  were set to  $10^{-5}$  and  $10^5$ , respectively.

---

<sup>1</sup>The compound *Conv(5, 20, 1, 0)/ReLU/MaxPool(2, 2, 0)* indicates a convolutional layer (*Conv*) using 20 filters of size  $5 \times 5$ , stride 1, and no padding, a nonlinear activation function (*ReLU*) and, a 2-D max-pooling layer with a channel of size  $2 \times 2$ , stride 2 and no padding. The syntax *FC(C)/Softmax* denotes a fully connected layer of  $C$  neurons followed by the *softmax* layer.

Table 3: Hyper-parameters for the experiments

	Hyper-parameters	$(G, \ell)$
ala	$\alpha \in \{10^{-1}, 10^{-\frac{1}{2}}, 1, 10^{\frac{1}{2}}, 10\},$	(0.3477, 0.1)
w1a	$\gamma_1 \in \{\frac{4}{G}, \frac{8}{G}, \frac{16}{G}, \frac{32}{G}\}, \gamma_2 \in \{\frac{1}{2G}, \frac{1}{G}, \frac{2}{G}\}$	(0.0887, 0.1)
cina		(0.0497, 0.1)
MNIST	$\alpha \in \{10^{-3}, 10^{-2}, 10^{-1}, 1\},$	(0.2517, 0.01)
CIFAR10	$\gamma_1 \in \{\frac{4}{G}, \frac{8}{G}, \frac{16}{G}\}, \gamma_2 \in \{\frac{1}{8G}, \frac{1}{4G}, \frac{1}{2G}\}$	(1.8375, 0.01)

Our experiments were carried out as in [7]. We ran the algorithms with varying settings of triplets  $(\alpha, \gamma_1, \gamma_2)$  whose values are given in Table 3 for each dataset. In the table we also report the value of  $G$  used for defining the triplets, that is the average norm of the stochastic gradients generated in a one-epoch run of the SGD method with a fixed learning rate  $\ell$ . We used 60 and 36 triplets for binary classification and multi-class problems, respectively. For the binary and multi-class test problems, given the triplet  $(\alpha, \gamma_1, \gamma_2)$ , we ran each algorithm 50 and 10 times using 50 and 10 predetermined random seeds, respectively. We present the testing accuracy, i.e., the percentage of samples in the testing set that the model correctly classifies; in case of multiple runs, the testing accuracy is averaged over the runs. In the figures shown in the following subsection, we use **ExIJK** to denote the results obtained in the Experiment where  $\alpha$ ,  $\gamma_1$ , and  $\gamma_2$  take the I-th, J-th, and K-th value indicated in Table 3, respectively.

In the solution of problems with logistic regression objective function, the initial guess was the zero vector,  $x_0 = 0$ . For solving the NN softmax cross-entropy problems, we used the Glorot (Xavier) initializer [40] for the weights, and zeros for the biases in the network’s layers. All algorithms terminated after five number of epochs, namely when the total number of single gradient evaluations  $\nabla f_i$ , reached or exceeded  $5N$ , where  $N$  is the number of training samples.

### 4.3. Numerical Results

We now present and analyze the numerical results obtained. Table 4 shows the percentage of unconstrained steps of the form  $p_k = -\mu_k g_k$  taken through the iterations within five epochs; the displayed data are averaged over the runs performed. We note that in some cases this percentage is equal to zero, thus the sequence of iterates  $\{x_k\}$  generated by our TRishBB variants coincides with the sequence generated by the first-order TRish. We also underline that the percentage of unconstrained steps increases with  $\alpha$ . In fact, taking into account the form of the steps (7), the larger  $\alpha$  is, the higher

Table 4: Percentage of BB steplengths taken with different  $\alpha$ 

ala	$\alpha = 10^{-1}$	$\alpha = 10^{-\frac{1}{2}}$	$\alpha = 1$	$\alpha = 10^{\frac{1}{2}}$	$\alpha = 10$
TRishBB_v1	00.83	50.00	81.67	92.50	98.33
TRishBB_v2	03.17	67.46	88.89	96.03	99.21
TRishBB_v3	00.00	03.96	05.56	21.43	60.31
wla	$\alpha = 10^{-1}$	$\alpha = 10^{-\frac{1}{2}}$	$\alpha = 1$	$\alpha = 10^{\frac{1}{2}}$	$\alpha = 10$
TRishBB_v1	03.80	11.96	27.72	61.62	79.35
TRishBB_v2	81.96	99.48	100	100	100
TRishBB_v3	02.06	03.09	05.67	09.79	16.49
cina	$\alpha = 10^{-1}$	$\alpha = 10^{-\frac{1}{2}}$	$\alpha = 1$	$\alpha = 10^{\frac{1}{2}}$	$\alpha = 10$
TRishBB_v1	14.11	60.08	88.04	90.59	89.65
TRishBB_v2	71.48	99.74	100	100	100
TRishBB_v3	00.13	00.77	03.20	33.33	72.12
MNIST	$\alpha = 10^{-3}$	$\alpha = 10^{-2}$	$\alpha = 10^{-1}$	$\alpha = 1$	
TRishBB_v1	00.00	00.36	66.67	96.10	
TRishBB_v2	00.00	00.00	00.13	87.88	
TRishBB_v3	00.00	00.00	00.00	00.34	
CIFAR10	$\alpha = 10^{-3}$	$\alpha = 10^{-2}$	$\alpha = 10^{-1}$	$\alpha = 1$	
TRishBB_v1	00.00	00.00	24.93	81.62	
TRishBB_v2	00.00	00.00	00.00	10.80	
TRishBB_v3	00.00	00.00	00.00	01.84	

the probability of taking unconstrained steps ( $-\mu_k g_k$ ) is; as a consequence the performance of TRishBB variants differ considerably from the performance of TRish for large values of  $\alpha$ .

In Table 5, averaging over the tested values of  $\gamma_1$  and  $\gamma_2$ , for every dataset and every value of  $\alpha$  we report the highest accuracy obtained by TRish and the variants of TRishBB; the reported values represent the largest accuracies among those reached at the end of each epoch. For each algorithm we also report the ratio (“accuracy ratio”) between the smallest and the largest accuracy reported in the corresponding line of the table. We can observe that the accuracy of TRishBB variants is comparable or higher than the accuracy of TRish and that the best results for TRishBB are obtained with the largest values of  $\alpha$  where it is possible to benefit of the BB steplengths for a large number of iterations. In order to give more insight on the behaviour of our three TRish variants in what follows we provide detailed statistics of the runs employing the largest value of  $\alpha$ .

Table 5: Highest testing accuracy with different  $\alpha$  (in %) and the accuracy ratio

ala	$\alpha = 10^{-1}$	$\alpha = 10^{-\frac{1}{2}}$	$\alpha = 1$	$\alpha = 10^{\frac{1}{2}}$	$\alpha = 10$	accuracy ratio
TRishBB_v1	83.76	83.55	83.09	82.54	82.40	0.9920
TRishBB_v2	83.87	83.67	83.52	83.52	83.52	0.9958
TRishBB_v3	83.75	83.51	81.66	79.69	80.27	0.9515
TRish	83.75	83.51	81.55	79.50	79.06	0.9440

wla	$\alpha = 10^{-1}$	$\alpha = 10^{-\frac{1}{2}}$	$\alpha = 1$	$\alpha = 10^{\frac{1}{2}}$	$\alpha = 10$	accuracy ratio
TRishBB_v1	89.61	89.67	89.57	89.23	88.83	0.9906
TRishBB_v2	89.59	89.58	89.57	89.57	89.57	0.9998
TRishBB_v3	89.62	89.67	89.57	89.29	88.94	0.9919
TRish	89.62	89.67	89.57	89.30	88.99	0.9924

cina	$\alpha = 10^{-1}$	$\alpha = 10^{-\frac{1}{2}}$	$\alpha = 1$	$\alpha = 10^{\frac{1}{2}}$	$\alpha = 10$	accuracy ratio
TRishBB_v1	91.70	91.63	91.37	90.84	90.29	0.9846
TRishBB_v2	91.49	91.45	91.45	91.45	91.45	0.9996
TRishBB_v3	91.64	91.68	90.83	89.36	90.46	0.9747
TRish	91.64	91.68	90.63	87.93	87.51	0.9545

MNIST	$\alpha = 10^{-3}$	$\alpha = 10^{-2}$	$\alpha = 10^{-1}$	$\alpha = 1$	accuracy ratio
TRishBB_v1	89.74	96.83	98.70	98.72	0.9090
TRishBB_v2	87.27	96.98	98.95	98.81	0.8820
TRishBB_v3	87.21	96.95	98.87	98.46	0.8821
TRish	87.21	96.95	98.87	98.42	0.8821

CIFAR10	$\alpha = 10^{-3}$	$\alpha = 10^{-2}$	$\alpha = 10^{-1}$	$\alpha = 1$	accuracy ratio
TRishBB_v1	30.86	44.72	59.19	65.41	0.4718
TRishBB_v2	31.15	44.95	60.74	65.98	0.4721
TRishBB_v3	31.09	45.05	60.37	64.60	0.4813
TRish	31.08	45.04	60.27	64.66	0.4807

#### 4.3.1. Datasets a1a, w1a, and cina

We present the averaged accuracies obtained with  $\alpha = 10$  for each of the five epochs performed in the experiments and for each triplet  $(\alpha, \gamma_1, \gamma_2) = (10, \gamma_1, \gamma_2)$ .

Figure 1–Figure 3 illustrate the results obtained on the dataset **a1a**. The results displayed indicate that the highest accuracy is achieved by TRishBB\_v2 in the first two epochs. The algorithms TRishBB\_v1 and TRishBB\_v2 outperform TRish, remarkably the testing accuracy reached is quite insensitive to the tested values of  $\gamma_1$  and  $\gamma_2$ . For large  $\alpha$ , these algorithms take the unconstrained step in the large majority of the iterations, see Table 4, and thus differ from TRish considerably. On the other hand, TRishBB\_v3 is generally more accurate than TRish but more sensitive to the choice of  $\gamma_1$  and  $\gamma_2$ ; the steplength  $\mu_k$  was selected approximately in 60% of the iterations.

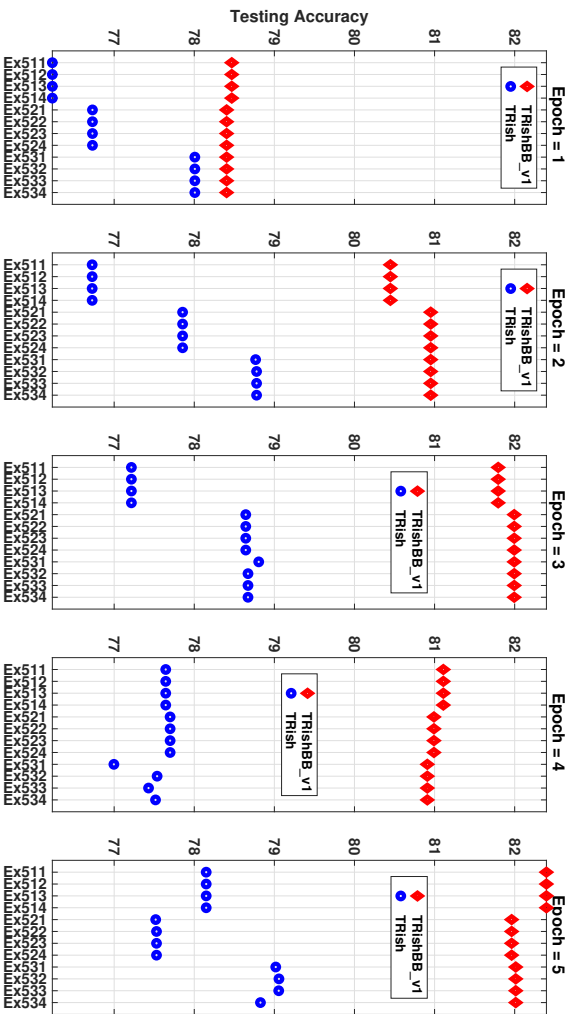


Figure 1: a1a: Average accuracy of TRishB-v1 with  $(\alpha, \gamma_1, \gamma_2) = (10, \gamma_1, \gamma_2)$ ,  $m = 20$ , and  $|M_k| = 64$ .

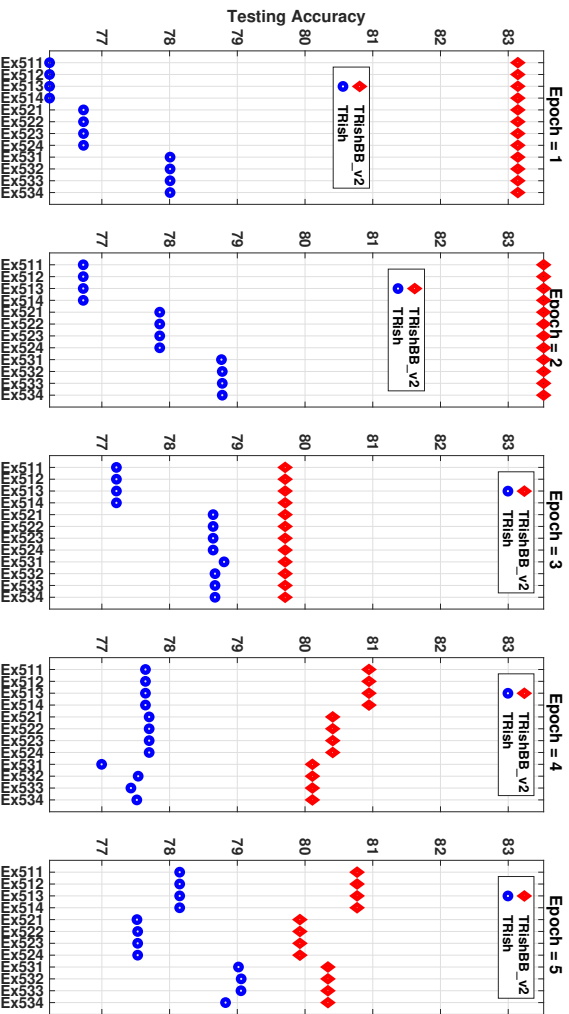


Figure 2: a1a: Average accuracy of TRishBB-v2 with  $(\alpha, \gamma_1, \gamma_2) = (10, \gamma_1, \gamma_2)$ ,  $m = N_b$ ,  $|M_k| = 64$ .

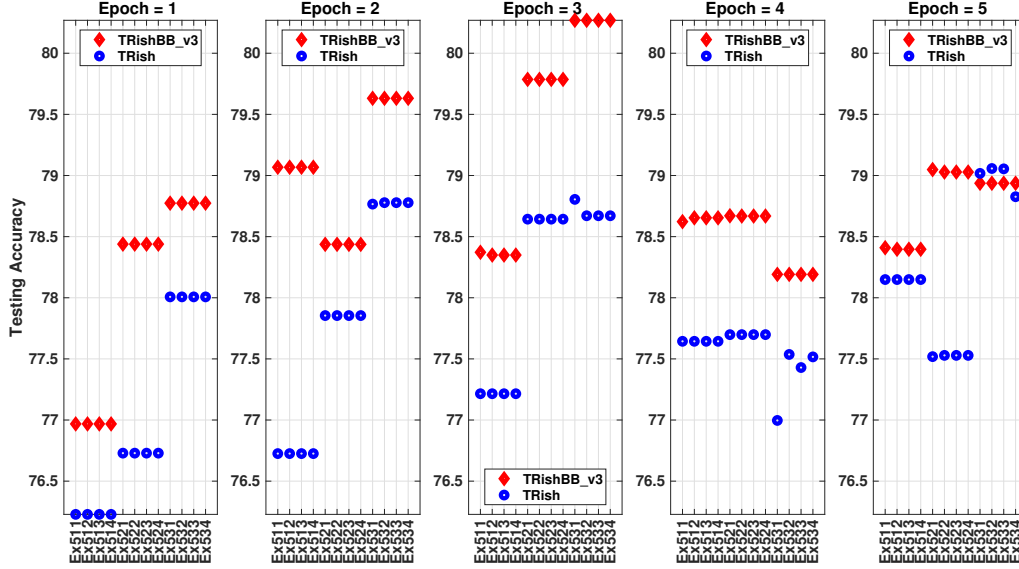


Figure 3: a1a: Average accuracy of TRishBB\_v3 with  $(\alpha, \gamma_1, \gamma_2) = (10, \gamma_1, \gamma_2)$ ,  $m = 5$ , and  $|\mathcal{N}_k| = 64$ .

Figure 4–Figure 6 concern the dataset `w1a`. Algorithm TRishBB\_v2 was very effective and its performance is insensitive to the triplet  $(\alpha, \gamma_1, \gamma_2) = (10, \gamma_1, \gamma_2)$  used. Using this triplet, the steplength  $\mu_k$  was selected at every iteration by this algorithm, see Table 4. On the other hand, the steplength  $\mu_k$  was selected approximately 79% and 16% of the iterations by TRishBB\_v1 and TRishBB\_v3 respectively. Algorithms TRishBB\_v1 and TRishBB\_v3 provided classification accuracies comparable to those of TRish.

Results for the dataset `cina` are displayed in Figure 7–Figure 9. From Table 4 we know that TRishBB\_v1 selected the steplength  $\mu_k$  approximately at the 89% of the iterations, TRishBB\_v2 selected  $\mu_k$  at all iterations while TRishBB\_v3 selected  $\mu_k$  around at the 72% of all iterations. TRishBB\_v1 is generally more accurate than TRish but more sensitive to the choice of  $\gamma_1$  and  $\gamma_2$  than TRishBB\_v2; Algorithm TRishBB\_v2 achieves high accuracy steadily for all the values  $\gamma_1$  and  $\gamma_2$ . Algorithm TRishBB\_v3 is the most sensitive to the values of  $\gamma_1$  and  $\gamma_2$ . From the second to the fifth epoch, it compares well with TRish but the accuracy is generally lower than the accuracy reached by TRishBB\_v2.

The results described above indicate that exploiting stochastic BB steplengths

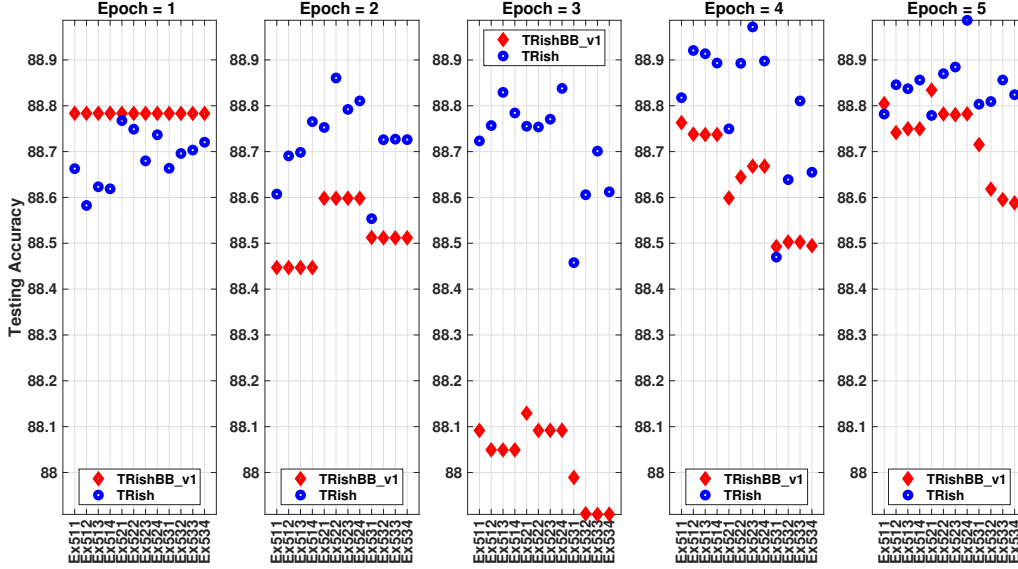


Figure 4: w1a: Average accuracy of TRishBB\_v1 with  $(\alpha, \gamma_1, \gamma_2) = (10, \gamma_1, \gamma_2)$ ,  $m = 20$ ,  $|\mathcal{N}_k| = 64$ .

and guidelines on stochastic quasi-Newton methods seems to considerably improve the overall performance of TRish. Algorithm TRishBB\_v2 provides the best accuracy and its performance is not affected by the specific triplet used. Figure 10 shows the average values of the BB parameters built with varying  $\gamma_1$  and  $\gamma_2$  for each dataset. It is evident that the rule for generating  $\mu_k$  in TRishBB\_v2 provides small values, thus enhancing the selection of unconstrained steps  $(-\mu_k g_k)$ . Coherently with the results above, the largest  $\mu_k$ 's are built in TRishBB\_v3.

#### 4.3.2. Datasets MNIST and CIFAR10

We present the averaged accuracies obtained for each of the five epochs performed in the experiments and for each triplet  $(\alpha, \gamma_1, \gamma_2) = (1, \gamma_1, \gamma_2)$ . As shown in Table 4, we first observe that the variants of TRishBB employed the unconstrained trust-region solution less frequently than for datasets (a1a, w1a, cina) but the percentage of unconstrained steps increases with the value of  $\alpha$ .

Figure 11–Figure 13 display the averaged accuracy obtained with the dataset MNIST. TRishBB\_v2 compares well with TRishBB\_v1 even though

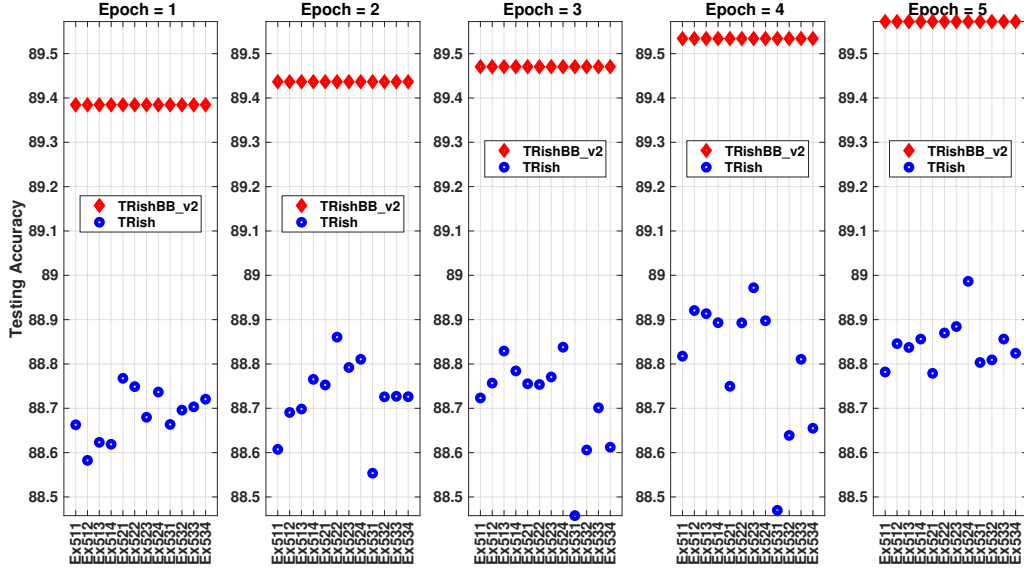


Figure 5: w1a: Average accuracy of TRishBB\_v2 with  $(\alpha, \gamma_1, \gamma_2) = (10, \gamma_1, \gamma_2)$ ,  $m = N_b$ ,  $|\mathcal{N}_k| = 64$ .

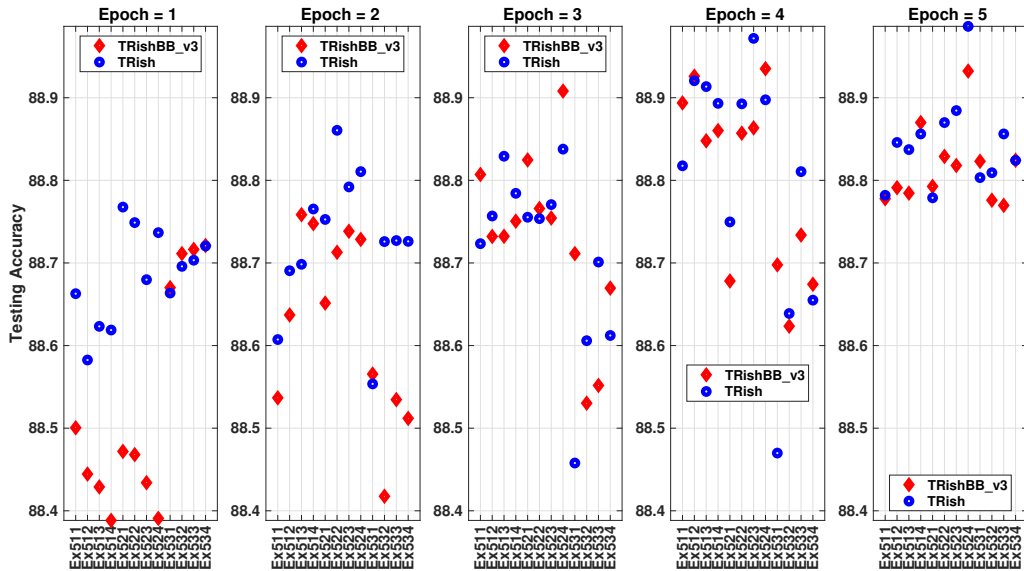


Figure 6: w1a: Average accuracy of TRishBB\_v3 with  $(\alpha, \gamma_1, \gamma_2) = (10, \gamma_1, \gamma_2)$ ,  $m = 5$ ,  $|\mathcal{N}_k| = 64$ .

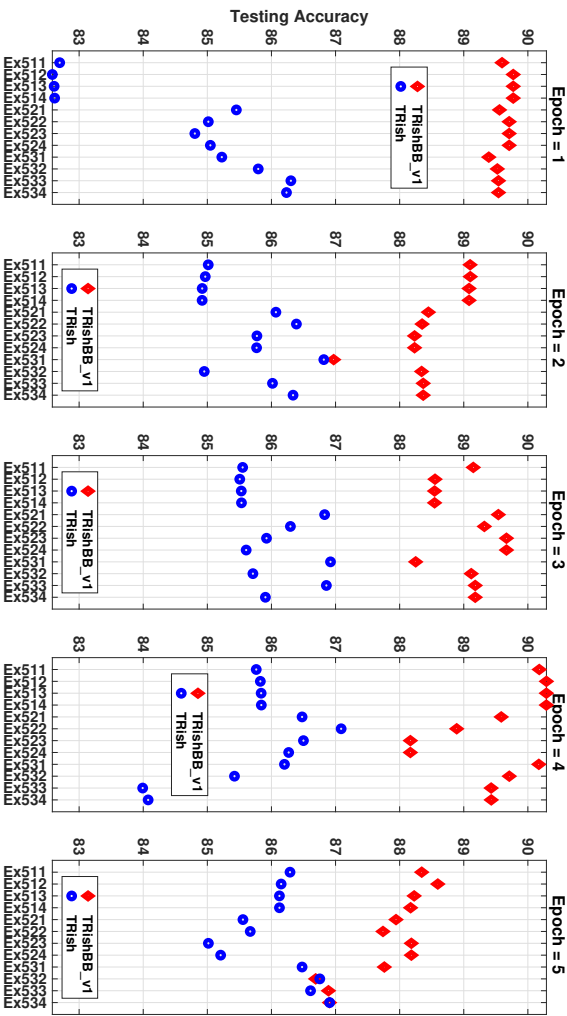


Figure 7: cina: Average accuracy of TRishBB-v1 with  $(\alpha, \gamma_1, \gamma_2) = (10, \gamma_1, \gamma_2)$ ,  $m = 20$ ,  $|\mathcal{N}_k| = 64$ .

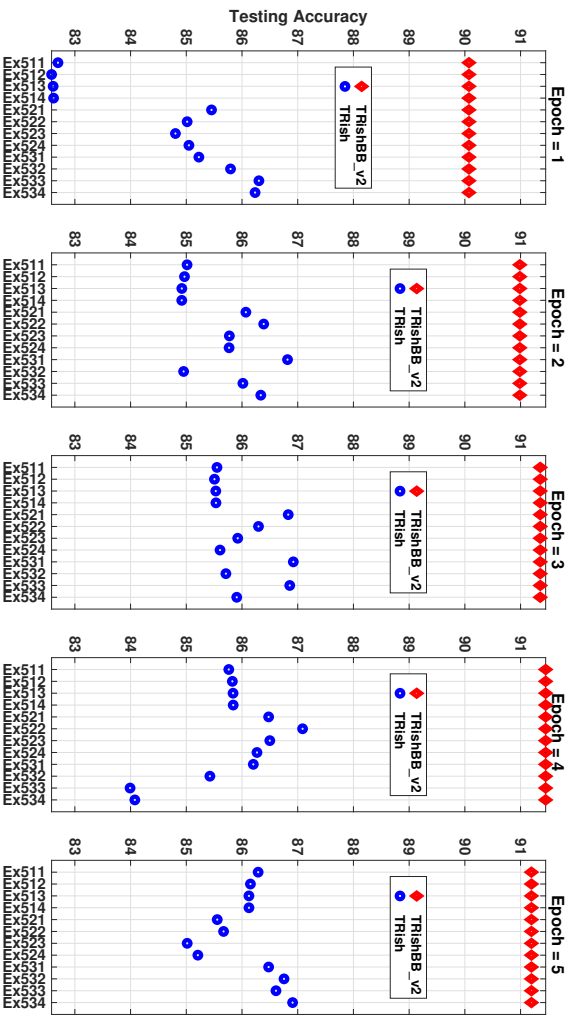


Figure 8: cina: Average accuracy of TRishBB-v2 with  $(\alpha, \gamma_1, \gamma_2) = (10, \gamma_1, \gamma_2)$ ,  $m = N_b$ ,  $|\mathcal{N}_k| = 64$ .

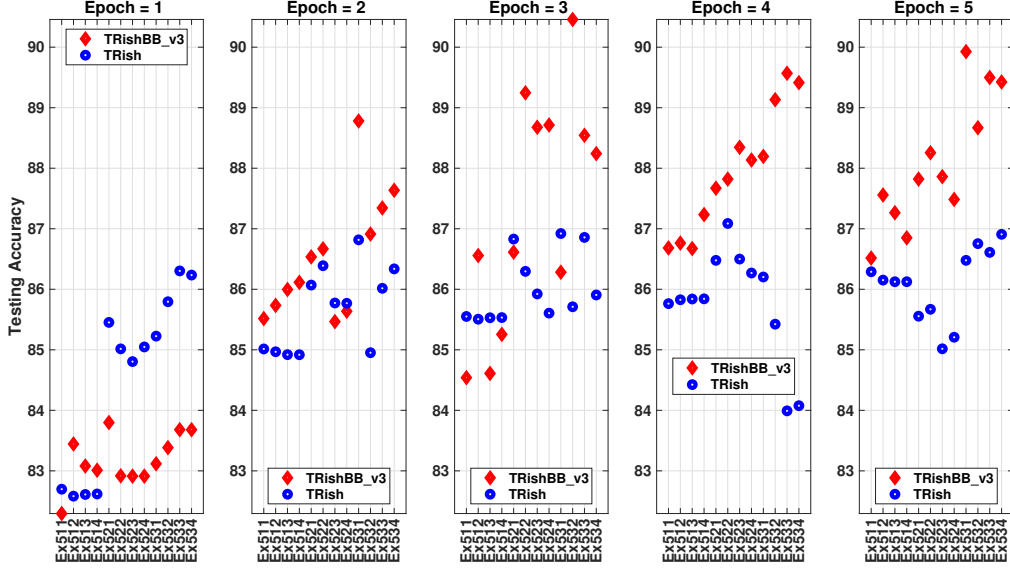


Figure 9: cina: Average accuracy of TRishBB\_v3 with  $(\alpha, \gamma_1, \gamma_2) = (10, \gamma_1, \gamma_2)$ ,  $m = 5$ ,  $|\mathcal{N}_k| = 64$

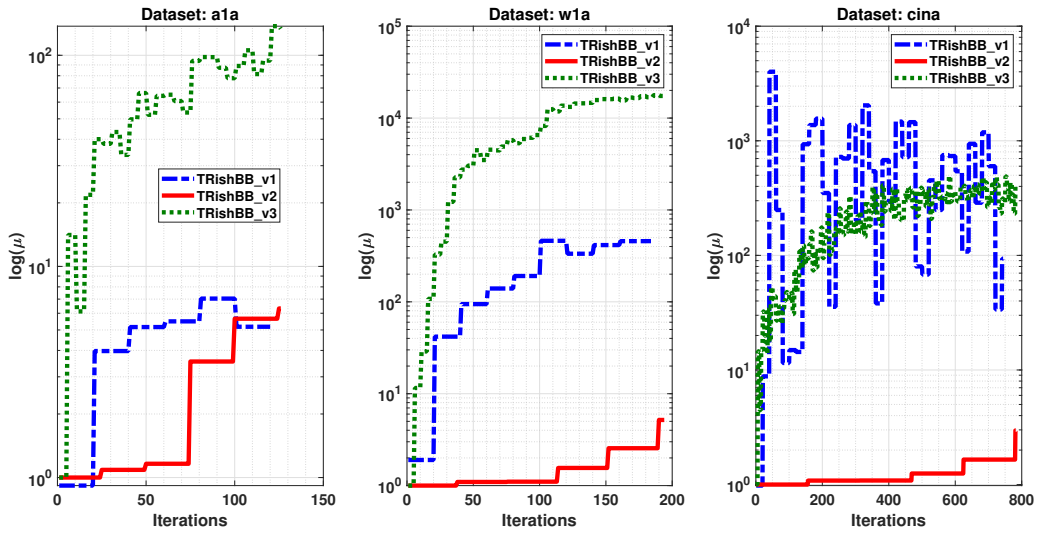


Figure 10: Average values of  $\mu_k$  with triplets  $(\alpha, \gamma_1, \gamma_2) = (10, \gamma_1, \gamma_2)$  along iterations for a1a, w1a and cina.

it employed a smaller percentage of unconstrained steps. Both TRishBB\_v1 and TRishBB\_v2 are quite insensitive to the values of  $\gamma_1$  and  $\gamma_2$ . TRishBB\_v3 selected the unconstrained steps less than 1% of the iterations and its performance is similar to the performance of TRish.

Figure 14–Figure 16 show the averaged accuracies with the dataset CIFAR10. The main observation is that the proposed TRishBB variants are less sensitive than TRish to the choice of  $\gamma_1$  and  $\gamma_2$ , see e.g., experiments Ex432 and Ex433. Except for the first epoch, TRishBB\_v2 performs better than TRish and than the other two variants. Algorithm TRishBB\_v1 generally performed better than Algorithm TRishBB\_v3 but it is not a clear winner against TRish. TRishBB\_v3 is again comparable to TRish since the percentage of unconstrained solution taken is less than 2%.

Figure 17 shows that the rule for generating  $\mu_k$  in TRishBB\_v2 yields small values. The values of  $\mu_k$  generated by TRishBB\_v1 are smaller than in TRishBB\_v2, in accordance with the high number of unconstrained steps taken by the two algorithms, but the overall results indicate that the rule for building the steplength  $\mu_k$  in TRishBB\_v2 is the most effective. The values of  $\mu_k$  built in TRishBB\_v3 are the largest at all iterations.

## 5. Conclusion

We introduced the Algorithm TRishBB applicable to finite-sum minimization problems. It is a stochastic trust-region method that combines the TRish methodology with stochastic Barzilai-Borwein steplengths to inject cheap second-order information. We presented theoretical analysis of TRishBB and devised three practical variants differing in the computation of the BB steplength. TRishBB\_v1 mimics the implementation of a standard BB rule, TRishBB\_v2 employs an accumulated BB parameter per iteration, TRishBB\_v3 retrieves the second-order information by the empirical Fisher Information matrix.

Numerical results demonstrated that TRishBB\_v2 is a reliable algorithm that outperforms the other variants and that it is quite insensitive to the choice of the hyperparameters  $\alpha$ ,  $\gamma_1$  and  $\gamma_2$ ; also for large value of the parameter  $\alpha$ , TRishBB\_v2 performs better than the first-order TRish method.

Regarding future investigations, it is worthy to further explore the definition of stochastic BB parameters, including stochastic diagonal BB rules, as suggested by [41].

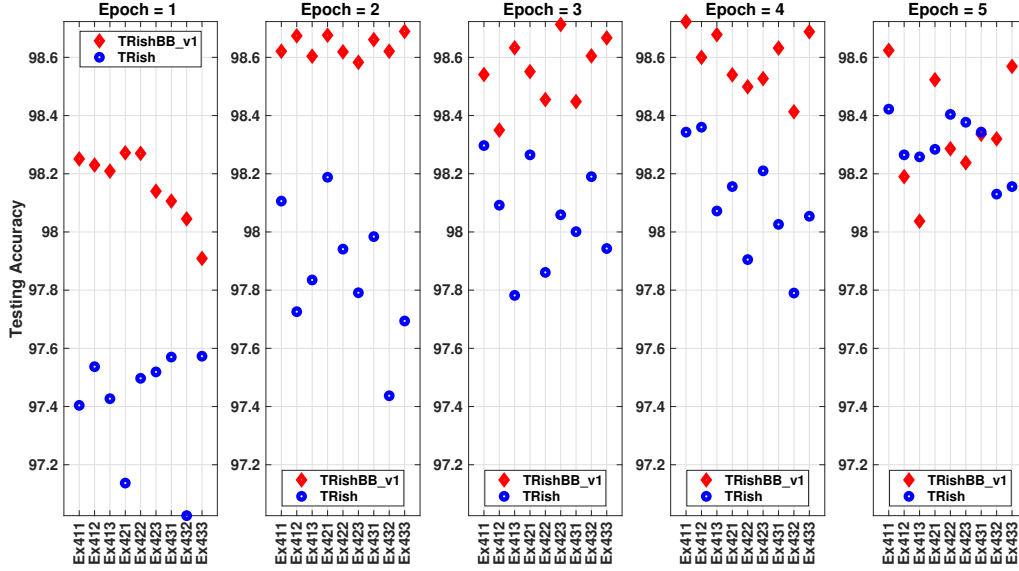


Figure 11: MNIST: Testing accuracy of TRishBB\_v1 with  $(\alpha, \gamma_1, \gamma_2) = (1, \gamma_1, \gamma_2)$ ,  $m = 20$ , and  $|\mathcal{N}_k| = 128$

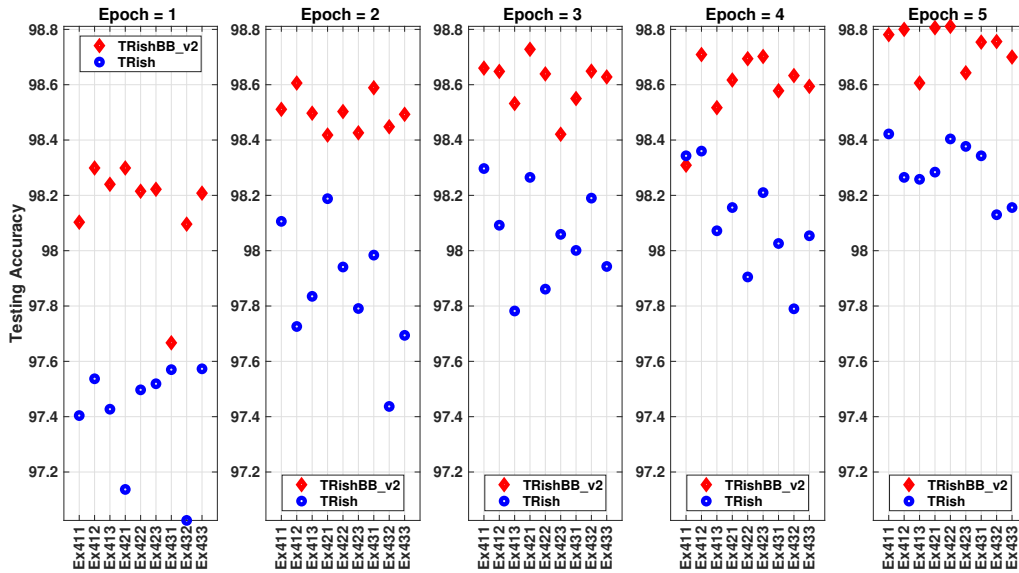


Figure 12: MNIST: Testing accuracy of TRishBB\_v2 with  $(\alpha, \gamma_1, \gamma_2) = (1, \gamma_1, \gamma_2)$ ,  $m = N_b$ , and  $|\mathcal{N}_k| = 128$  using damping relaxed combination

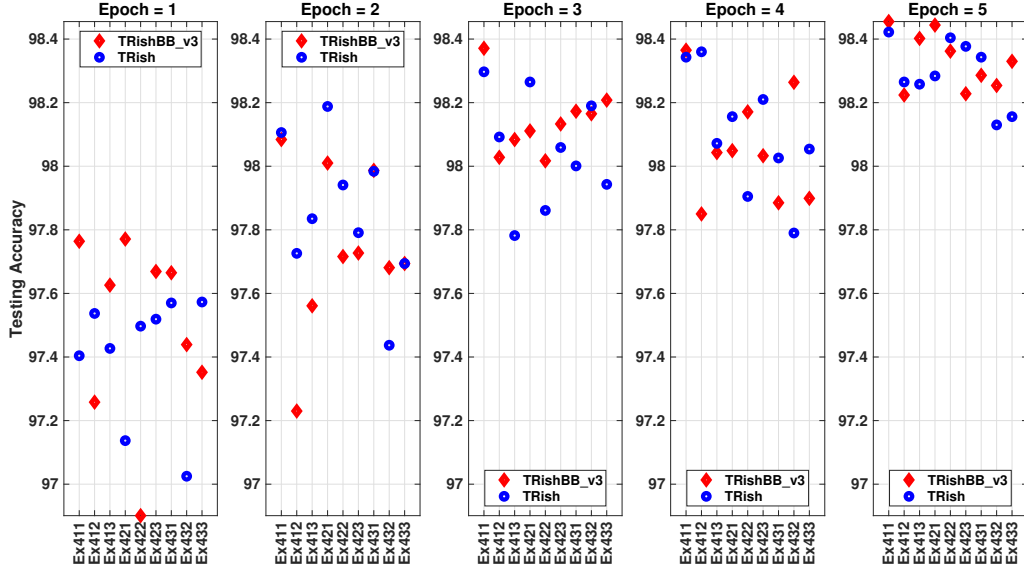


Figure 13: MNIST: Testing accuracy of TRishBB\_v3 with  $(\alpha, \gamma_1, \gamma_2) = (1, \gamma_1, \gamma_2)$ ,  $m = 5$ , and  $|\mathcal{N}_k| = 128$

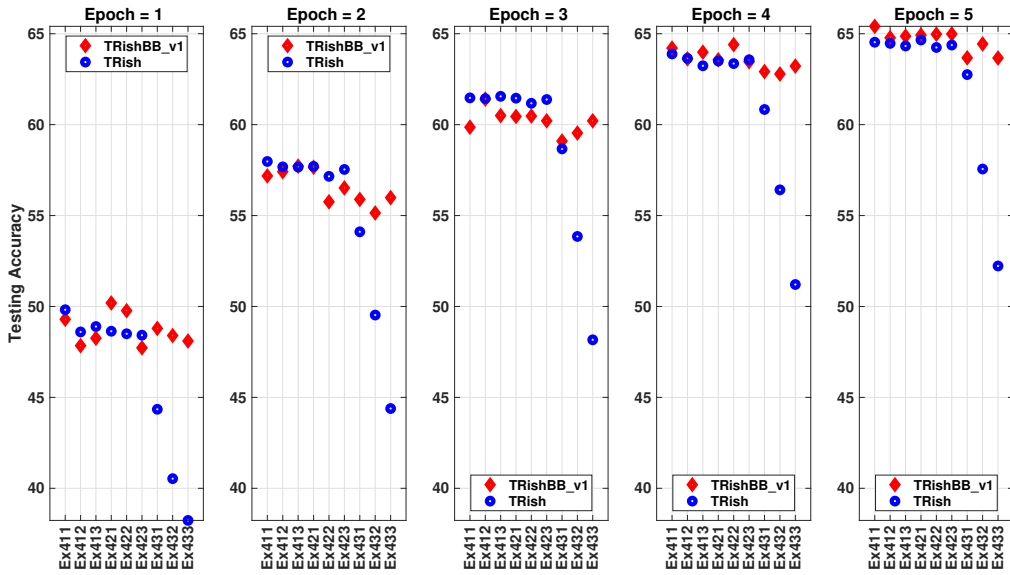


Figure 14: CIFAR10: Testing accuracy of TRishBB\_v1 with  $(\alpha, \gamma_1, \gamma_2) = (1, \gamma_1, \gamma_2)$ ,  $m = 20$ , and  $|\mathcal{N}_k| = 128$

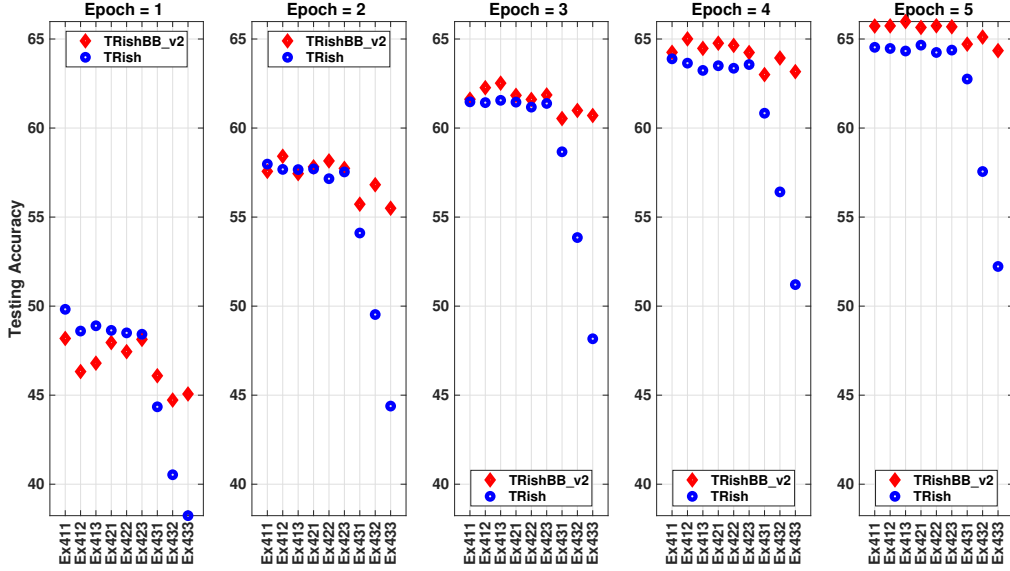


Figure 15: CIFAR10: Testing accuracy of TRishBB\_v2 with  $(\alpha, \gamma_1, \gamma_2) = (1, \gamma_1, \gamma_2)$ ,  $m = N_b$ , and  $|\mathcal{N}_k| = 128$  using damping relaxed combination

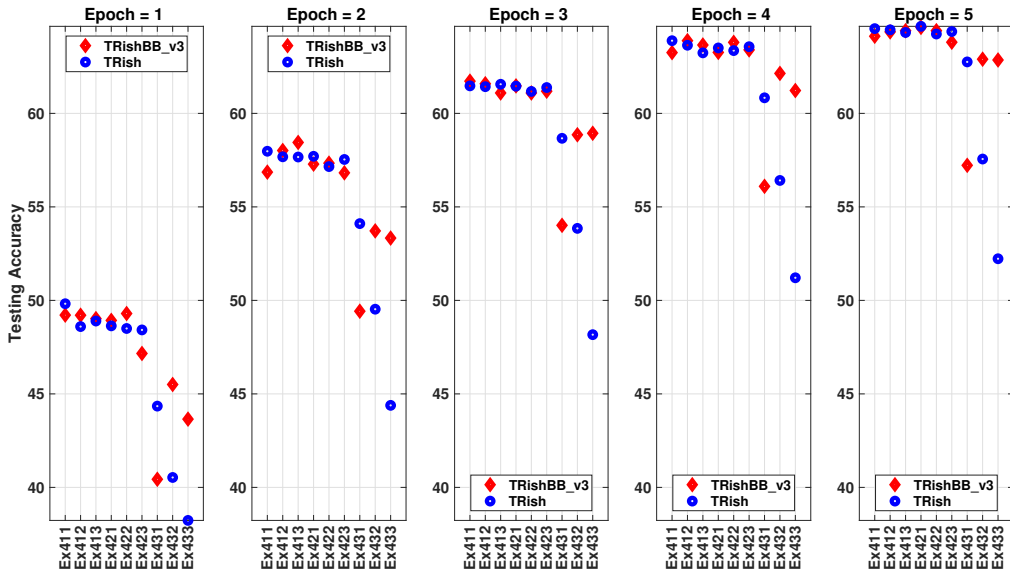


Figure 16: CIFAR10: Testing accuracy of TRishBB\_v3 with  $(\alpha, \gamma_1, \gamma_2) = (1, \gamma_1, \gamma_2)$ ,  $m = 5$ , and  $|\mathcal{N}_k| = 128$

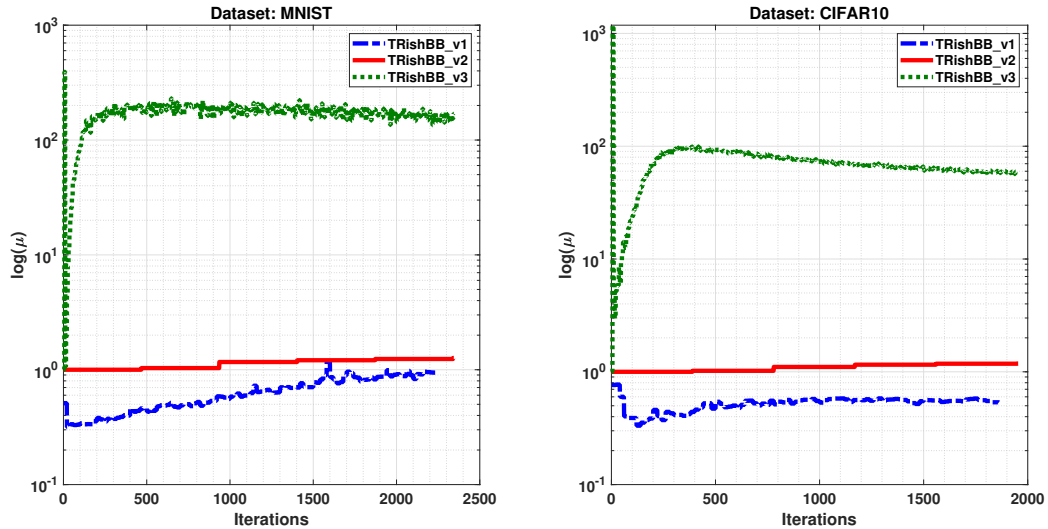


Figure 17: Average values of  $\mu_k$  with triplets  $(\alpha, \gamma_1, \gamma_2) = (1, \gamma_1, \gamma_2)$  along iterations for MNIST and CIFAR10.

## A. Some intermediate results

We present some theoretical results required in Appendix B.

**Lemma A.1.** *Suppose Assumption 3.1 holds, then*

$$f(x_{k+1}) - f(x_k) \leq \underbrace{g_k^T p_k + \frac{1}{2\mu_k} \|p_k\|^2}_{m_k(p_k)} + (\nabla f(x_k) - g_k)^T p_k + \frac{L}{2} \|p_k\|^2. \quad (\text{A.1})$$

*Proof.* By (10), we have

$$f(x_{k+1}) - f(x_k) \leq \nabla f(x_k)^T p_k + \frac{L}{2} \|p_k\|^2.$$

Adding, subtracting  $g_k^T p_k$ , and using the fact that  $\frac{1}{2\mu_k} \|p_k\|^2 \geq 0$  conclude the proof.  $\square$

**Lemma A.2.** *Suppose Assumption 3.1 holds, then*

$$m_k(p_k) = g_k^T p_k + \frac{1}{2\mu_k} \|p_k\|^2 \leq -\Delta_k \|g_k\| + \frac{1}{2\mu_k} \Delta_k^2. \quad (\text{A.2})$$

*Proof.* If  $p_k = -\mu_k g_k$ , then  $m_k(p_k) = -\frac{1}{2}\mu_k \|g_k\|^2$ . If  $p_k = -\frac{\Delta_k}{\|g_k\|} g_k$ , then  $m_k(p_k) = -\Delta_k \|g_k\| + \frac{1}{2\mu_k} \Delta_k^2$ . Since  $m_k(-\mu g_k)$  is the minimum value attainable by  $m_k$ , the proof is concluded.  $\square$

## B. Proofs from §Section 3

### B.1. PROOF OF LEMMA 3.1

*Proof.* Given the step taken by the Algorithm 1, i.e.,  $p_k = x_{k+1} - x_k$ , the inequality (10) implies

$$f(x_{k+1}) = f(x_k + p_k) \leq f(x_k) + \nabla f(x_k)^T p_k + \frac{L}{2} \|p_k\|^2. \quad (\text{B.1})$$

Thus, considering the events that Case 1–3 occur, i.e.,  $C_{i,k}$  for  $i = 1, 2, 3$ , the law of total probability gives

$$\begin{aligned} \mathbb{E}_k[f(x_{k+1})] - f(x_k) &\leq \mathbb{E}_k[\nabla f(x_k)^T p_k] + \frac{L}{2} \mathbb{E}_k[\|p_k\|^2] \\ &= \sum_{i=1}^3 \mathbb{P}_k[C_{i,k}] \mathbb{E}_k[\nabla f(x_k)^T p_k | C_{i,k}] + \frac{L}{2} \sum_{i=1}^3 \mathbb{P}_k[C_{i,k}] \mathbb{E}_k[\|p_k\|^2 | C_{i,k}]. \end{aligned} \quad (\text{B.2})$$

Further,

$$\begin{aligned} \mathbb{E}_k[\nabla f(x_k)^T p_k | C_{i,k}] &= \mathbb{P}_k[\overline{S_{BB}} | C_{i,k}] \mathbb{E}_k[\nabla f(x_k)^T p_k | C_{i,k} \cap \overline{S_{BB}}] \\ &\quad + \mathbb{P}_k[S_{BB} | C_{i,k}] \mathbb{E}_k[\nabla f(x_k)^T p_k | C_{i,k} \cap S_{BB}], \end{aligned} \quad (\text{B.3})$$

and

$$\begin{aligned} \mathbb{E}_k[\|p_k\|^2 | C_{i,k}] &= \mathbb{P}_k[\overline{S_{BB}} | C_{i,k}] \mathbb{E}_k[\|p_k\|^2 | C_{i,k} \cap \overline{S_{BB}}] \\ &\quad + \mathbb{P}_k[S_{BB} | C_{i,k}] \mathbb{E}_k[\|p_k\|^2 | C_{i,k} \cap S_{BB}], \end{aligned} \quad (\text{B.4})$$

for  $i = 1, 2, 3$ . Now, we analyze the events separately.

**EVENT  $C_{1,k}$ .** Consider the event  $\overline{C_{1,k}^{BB}} \stackrel{\text{def}}{=} C_{1,k} \cap \overline{S_{BB}}$ . It holds  $p_k = -\gamma_1 \alpha g_k$ , and [7, Equations (8), (9)] gives

$$\begin{aligned} \mathbb{E}_k[\nabla f(x_k)^T p_k | \overline{C_{1,k}^{BB}}] &\leq -\gamma_1 \alpha \mathbb{E}_k \left[ \nabla f(x_k)^T g_k | \overline{C_{1,k}^{BB}} \right] \\ &\quad + (\gamma_1 - \gamma_2) \alpha \mathbb{P}_k \left[ \mathcal{E}_k | \overline{C_{1,k}^{BB}} \right] \mathbb{E}_k \left[ \nabla f(x_k)^T g_k | \overline{C_{1,k}^{BB}} \cap \mathcal{E}_k \right], \end{aligned}$$

and

$$\mathbb{E}_k \left[ \|p_k\|^2 | \overline{C_{1,k}^{BB}} \right] = \gamma_1^2 \alpha^2 \mathbb{E}_k \left[ \|g_k\|^2 | \overline{C_{1,k}^{BB}} \right].$$

In the event  $C_{1,k}^{BB} \stackrel{\text{def}}{=} C_{1,k} \cap S_{BB}$ , it holds  $p_k = -\mu_k g_k$  with  $\mu_k \leq \gamma_1 \alpha$ , and paralleling [7, Equations (8) and (9)] results in

$$\begin{aligned} \mathbb{E}_k [\nabla f(x_k)^T p_k | C_{1,k}^{BB}] &= \mathbb{E}_k [-\mu_k \nabla f(x_k)^T g_k | C_{1,k}^{BB}] \\ &\leq (\gamma_1 \alpha - \mu_{\min}) \mathbb{P}_k [\mathcal{E}_k | C_{1,k}^{BB}] \mathbb{E}_k [\nabla f(x_k)^T g_k | C_{1,k}^{BB} \cap \mathcal{E}_k] \\ &\quad - \gamma_1 \alpha \mathbb{E}_k [\nabla f(x_k)^T g_k | C_{1,k}^{BB}], \end{aligned}$$

and

$$\mathbb{E}_k [\|p_k\|^2 | C_{1,k}^{BB}] \leq \gamma_1^2 \alpha^2 \mathbb{E}_k [\|g_k\|^2 | C_{1,k}^{BB}].$$

Now, we combine (B.3), (B.4) and the previous results. We take into account that  $(\gamma_1 - \gamma_2)\alpha \leq (\gamma_1 \alpha - \mu_{\min})$  by Assumption 3.4 and

$$\mathbb{P}_k (\mathcal{E}_k | \overline{C_{1,k}^{BB}}) \leq \mathbb{P}_k (\mathcal{E}_k | C_{1,k}), \quad \mathbb{P}_k (\mathcal{E}_k | C_{1,k}^{BB}) \leq \mathbb{P}_k (\mathcal{E}_k | C_{1,k}).$$

Thus, we get

$$\begin{aligned} \mathbb{E}_k [\nabla f(x_k)^T p_k | C_{1,k}] &\leq (\gamma_1 \alpha - \mu_{\min}) \mathbb{P}_k [S_{BB} | C_{1,k}] \mathbb{P}_k (\mathcal{E}_k | C_{1,k}^{BB}) \mathbb{E}_k [\nabla f(x_k)^T g_k | C_{1,k}^{BB} \cap \mathcal{E}_k] \\ &\quad - \gamma_1 \alpha \left( \mathbb{P}_k [\overline{S_{BB}} | C_{1,k}] \mathbb{E}_k [\nabla f(x_k)^T g_k | \overline{C_{1,k}^{BB}}] + \mathbb{P}_k [S_{BB} | C_{1,k}] \mathbb{E}_k [\nabla f(x_k)^T g_k | C_{1,k}^{BB}] \right) \\ &\quad + (\gamma_1 \alpha - \mu_{\min}) \left( \mathbb{P}_k [\overline{S_{BB}} | C_{1,k}] \mathbb{P}_k [\mathcal{E}_k | \overline{C_{1,k}^{BB}}] \mathbb{E}_k [\nabla f(x_k)^T g_k | \overline{C_{1,k}^{BB}} \cap \mathcal{E}_k], \right. \end{aligned}$$

i.e.,

$$\begin{aligned} \mathbb{E}_k [\nabla f(x_k)^T p_k | C_{1,k}] &\leq (\gamma_1 \alpha - \mu_{\min}) \mathbb{P}_k (\mathcal{E}_k | C_{1,k}) \mathbb{E}_k [\nabla f(x_k)^T g_k | C_{1,k} \cap \mathcal{E}_k] \\ &\quad - \gamma_1 \alpha \mathbb{E}_k [\nabla f(x_k)^T g_k | C_{1,k}], \end{aligned}$$

and

$$\mathbb{E}_k [\|p_k\|^2 | C_{1,k}] \leq \gamma_1^2 \alpha^2 \mathbb{E}_k [\|g_k\|^2 | C_{1,k}]. \quad (\text{B.5})$$

EVENT  $C_{2,k}$ . The event  $C_{2,k}$  occurs when  $\|g_k\|^{-1} \leq \gamma_1$  and  $\|g_k\|^{-1} \geq \gamma_2$ . In the event  $\overline{C_{2,k}^{BB}} \stackrel{\text{def}}{=} C_{2,k} \cap \overline{S_{BB}}$ , it holds  $p_k = -\alpha g_k / \|g_k\|$  and [7, Equations (10) and (11)] gives

$$\begin{aligned} \mathbb{E}_k [\nabla f(x_k)^T p_k | \overline{C_{2,k}^{BB}}] &\leq -\gamma_1 \alpha \mathbb{E}_k \left[ \nabla f(x_k)^T g_k | \overline{C_{2,k}^{BB}} \right] \\ &\quad + (\gamma_1 - \gamma_2) \alpha \mathbb{P}_k \left[ \mathcal{E}_k | \overline{C_{2,k}^{BB}} \right] \mathbb{E}_k \left[ \nabla f(x_k)^T g_k | \overline{C_{2,k}^{BB}} \cap \mathcal{E}_k \right] \end{aligned}$$

and

$$\mathbb{E}_k \left[ \|p_k\|^2 | \overline{C_{2,k}^{BB}} \right] = \alpha^2 \leq \gamma_1^2 \alpha^2 \mathbb{E}_k \left[ \|g_k\|^2 | \overline{C_{2,k}^{BB}} \right].$$

Assumption 3.4 ensures that  $\mu_{min} \leq \frac{\alpha}{\|g_k\|}$  and in the event  $C_{2,k}^{BB} \stackrel{\text{def}}{=} C_{2,k} \cap S_{BB}$ , it holds  $\mu_{min} \leq \mu_k \leq \frac{\alpha}{\|g_k\|}$ . Then,

$$\begin{aligned} \mathbb{E}_k \left[ \nabla f(x_k)^T p_k | C_{2,k}^{BB} \right] &\leq -\mu_{min} \mathbb{P}_k \left[ \mathcal{E}_k | C_{2,k}^{BB} \right] \mathbb{E}_k \left[ \nabla f(x_k)^T g_k | C_{2,k}^{BB} \cap \mathcal{E}_k \right] \\ &\quad - \alpha \mathbb{P}_k \left[ \overline{\mathcal{E}_k} | C_{2,k}^{BB} \right] \mathbb{E}_k \left[ \frac{\nabla f(x_k)^T g_k}{\|g_k\|} | C_{2,k}^{BB} \cap \overline{\mathcal{E}_k} \right] \\ &\leq -\mu_{min} \mathbb{P}_k \left[ \mathcal{E}_k | C_{2,k}^{BB} \right] \mathbb{E}_k \left[ \nabla f(x_k)^T g_k | C_{2,k}^{BB} \cap \mathcal{E}_k \right] \\ &\quad - \gamma_1 \alpha \mathbb{P}_k \left[ \overline{\mathcal{E}_k} | C_{2,k}^{BB} \right] \mathbb{E}_k \left[ \nabla f(x_k)^T g_k | C_{2,k}^{BB} \cap \overline{\mathcal{E}_k} \right] \\ &= -\gamma_1 \alpha \mathbb{E}_k \left[ \nabla f(x_k)^T g_k | C_{2,k}^{BB} \right] \\ &\quad + (\gamma_1 \alpha - \mu_{min}) \mathbb{P}_k \left[ \mathcal{E}_k | C_{2,k}^{BB} \right] \mathbb{E}_k \left[ \nabla f(x_k)^T g_k | C_{2,k}^{BB} \cap \mathcal{E}_k \right], \end{aligned}$$

and

$$\mathbb{E}_k \left[ \|p_k\|^2 | C_{2,k}^{BB} \right] \leq \alpha^2 \leq \gamma_1^2 \alpha^2 \mathbb{E}_k \left[ \|g_k\|^2 | C_{2,k}^{BB} \right].$$

Now, we combine (B.3), (B.4) and the previous results. We take into account that  $(\gamma_1 - \gamma_2)\alpha \leq (\gamma_1 \alpha - \mu_{min})$  by Assumption 3.4 and that

$$\mathbb{P}_k \left( \mathcal{E}_k | \overline{C_{2,k}^{BB}} \right) \leq \mathbb{P}_k \left( \mathcal{E}_k | C_{2,k} \right), \quad \mathbb{P}_k \left( \mathcal{E}_k | C_{2,k}^{BB} \right) \leq \mathbb{P}_k \left( \mathcal{E}_k | C_{2,k} \right).$$

It follows

$$\begin{aligned} \mathbb{E}_k \left[ \nabla f(x_k)^T p_k | C_{2,k} \right] &\leq -\gamma_1 \alpha \left( \mathbb{P}_k \left[ \overline{S_{BB}} | C_{2,k} \right] \mathbb{E}_k \left[ \nabla f(x_k)^T p_k | \overline{C_{2,k}^{BB}} \right] \right. \\ &\quad \left. + \mathbb{P}_k \left[ S_{BB} | C_{2,k} \right] \mathbb{E}_k \left[ \nabla f(x_k)^T p_k | C_{2,k}^{BB} \right] \right) \\ &\quad + (\gamma_1 \alpha - \mu_{min}) \left( \mathbb{P}_k \left[ \overline{S_{BB}} | C_{2,k} \right] \mathbb{P}_k \left[ \mathcal{E}_k | C_{2,k} \cap \overline{S_{BB}} \right] \mathbb{E}_k \left[ \nabla f(x_k)^T p_k | \overline{C_{2,k}^{BB}} \cap \mathcal{E}_k \right] \right. \\ &\quad \left. + \mathbb{P}_k \left[ S_{BB} | C_{2,k} \right] \mathbb{P}_k \left[ \mathcal{E}_k | C_{2,k}^{BB} \right] \mathbb{E}_k \left[ \nabla f(x_k)^T p_k | C_{2,k}^{BB} \cap \mathcal{E}_k \right] \right), \end{aligned}$$

and finally

$$\begin{aligned} \mathbb{E}_k \left[ \nabla f(x_k)^T p_k | C_{2,k} \right] &\leq (\gamma_1 \alpha - \mu_{min}) \mathbb{P}_k \left( \mathcal{E}_k | C_{2,k} \right) \mathbb{E}_k \left[ \nabla f(x_k)^T p_k | C_{2,k} \cap \mathcal{E}_k \right] \\ &\quad - \gamma_1 \alpha \mathbb{E}_k \left[ \nabla f(x_k)^T p_k | C_{2,k} \right]. \end{aligned} \tag{B.6}$$

Further,

$$\mathbb{E}_k[\|p_k\|^2|C_{2,k}] \leq \alpha^2 \leq \gamma_1^2 \alpha^2 \mathbb{E}_k[\|g_k\|^2|C_{2,k}]. \quad (\text{B.7})$$

EVENT  $C_{3,k}$ . Following [7, Equations (12) and (13)] and the lines of the proof for the event  $C_{1,k}$ , we obtain

$$\begin{aligned} \mathbb{E}_k[\nabla f(x_k)^T p_k | C_{3,k}] &\leq (\gamma_1 \alpha - \mu_{min}) \mathbb{P}_k(\mathcal{E}_k | C_{3,k}) \mathbb{E}_k[\nabla f(x_k)^T g_k | C_{3,k} \cap \mathcal{E}_k] \\ &\quad - \gamma_1 \alpha \mathbb{E}_k[\nabla f(x_k)^T g_k | C_{3,k}], \end{aligned} \quad (\text{B.8})$$

and

$$\mathbb{E}_k[\|p_k\|^2 | C_{3,k}] \leq \gamma_1^2 \alpha^2 \mathbb{E}_k[\|g_k\|^2 | C_{3,k}]. \quad (\text{B.9})$$

Combining (B.2), (B.8) and (B.9), the claim follows.  $\square$

### B.2. PROOF OF LEMMA 3.3

*Proof.* Regarding (29), we analyze the different events  $C_{1,k}$ ,  $i = 1, 2, 3$ , separately.

EVENT  $C_{1,k}$ . Since  $\Delta_k = \gamma_1 \alpha \|g_k\|$ , the rightmost inequality in (35) and (A.2) give

$$m_k(p_k) \leq -\gamma_1 \alpha \left(1 - \frac{1}{2} \frac{\gamma_1 \alpha}{\mu_k}\right) \|g_k\|^2 \leq -\frac{3}{8} \gamma_1 \alpha \|g_k\|^2.$$

Using  $\|p_k\| \leq \gamma_1 \alpha \|g_k\|$ , Lemma A.1, the leftmost inequality in (35) and  $\gamma_1 \geq \gamma_2$ , we find that

$$\begin{aligned} &f(x_{k+1}) - f(x_k) \\ &\leq -\frac{3}{8} \gamma_1 \alpha \|g_k\|^2 + \gamma_1 \alpha \|\nabla f(x_k) - g_k\| \|g_k\| + \frac{1}{2} L \gamma_1^2 \alpha^2 \|g_k\|^2 \\ &\leq -\frac{3}{8} \gamma_1 \alpha \|g_k\|^2 + \gamma_1 \alpha \|\nabla f(x_k) - g_k\| \|g_k\| + \frac{1}{16} \gamma_1 \alpha \|g_k\|^2. \end{aligned}$$

Then, by  $\gamma_1 \geq \gamma_2$  and

$$0 \leq \left(\frac{1}{2} \|g_k\| - \|\nabla f(x_k) - g_k\|\right)^2 = \frac{1}{4} \|g_k\|^2 - \|\nabla f(x_k) - g_k\| \|g_k\| + \|\nabla f(x_k) - g_k\|^2,$$

we obtain

$$\begin{aligned} &f(x_{k+1}) - f(x_k) \\ &\leq -\frac{1}{16} \gamma_1 \alpha \|g_k\|^2 + \gamma_1 \alpha \|\nabla f(x_k) - g_k\|^2 \\ &\leq -\frac{1}{16} \gamma_2 \alpha \|g_k\|^2 + \frac{\gamma_1^2}{\gamma_2} \alpha \|\nabla f(x_k) - g_k\|^2. \end{aligned} \quad (\text{B.10})$$

EVENT  $C_{2,k}$ . Since  $\Delta_k = \alpha$ , using (A.2), the rightmost inequality in (35) and  $1/\gamma_1 \leq \|g_k\| \leq 1/\gamma_2$  gives

$$m_k(p_k) \leq -\alpha\|g_k\| + \frac{1}{2}\frac{\alpha^2}{\mu_k} \leq -\alpha\|g_k\| + \frac{5}{8}\frac{\alpha}{\gamma_1} \leq -\frac{3}{8}\alpha\|g_k\| \leq -\frac{3}{8}\gamma_2\alpha\|g_k\|^2.$$

Using  $1/\gamma_1 \leq \|g_k\| \leq 1/\gamma_2$ , Lemma A.1, and the leftmost inequality in (35), we find that

$$\begin{aligned} f(x_{k+1}) - f(x_k) &\leq -\frac{3}{8}\gamma_2\alpha\|g_k\|^2 + \|\nabla f(x_k) - g_k\|\alpha + \frac{1}{2}L\alpha^2 \\ &\leq -\frac{3}{8}\gamma_2\alpha\|g_k\|^2 + \|\nabla f(x_k) - g_k\|\alpha + \frac{1}{2}\gamma_1^2\alpha^2L\|g_k\|^2 \\ &\leq -\frac{3}{8}\gamma_2\alpha\|g_k\|^2 + \|\nabla f(x_k) - g_k\|\alpha + \frac{1}{16}\gamma_2\alpha\|g_k\|^2. \end{aligned}$$

Since

$$0 \leq \frac{\gamma_2}{\gamma_1^2} \left( \frac{1}{2} - \frac{\gamma_1^2}{\gamma_2} \|\nabla f(x_k) - g_k\| \right)^2 = \frac{\gamma_2}{4\gamma_1^2} - \|\nabla f(x_k) - g_k\| + \frac{\gamma_1^2}{\gamma_2} \|\nabla f(x_k) - g_k\|^2,$$

we obtain

$$f(x_{k+1}) - f(x_k) \leq -\frac{1}{16}\gamma_2\alpha\|g_k\|^2 + \frac{\gamma_1^2}{\gamma_2}\alpha\|\nabla f(x_k) - g_k\|^2.$$

EVENT  $C_{3,k}$ . The proof trivially follows what we argued for the event  $C_{1,k}$  as we have  $\gamma_1 \geq \gamma_2$ .

Summarizing the analysis above, inequality (29) holds. Finally, regarding (30), due to (26) and (27), inequality (29) yields

$$\begin{aligned} &\mathbb{E}_k[f(x_{k+1})] - f(x_k) \\ &\leq -\frac{1}{16}\gamma_2\alpha(\|\nabla f(x_k)\|^2 + \mathbb{E}_k[\|\nabla f(x_k) - g_k\|^2]) + \frac{\gamma_1^2}{\gamma_2}\alpha\mathbb{E}_k[\|\nabla f(x_k) - g_k\|^2] \\ &= -\frac{1}{16}\gamma_2\alpha\|\nabla f(x_k)\|^2 + \alpha \left( \frac{\gamma_1^2}{\gamma_2} - \frac{1}{16}\gamma_2 \right) \mathbb{E}_k[\|\nabla f(x_k) - g_k\|^2] \end{aligned}$$

which give the thesis.  $\square$

## Acknowledgments

The authors are members of the INdAM-GNCS Research Group. This research was partially supported by INDAM-GNCS through Progetti di Ricerca 2023, by PNRR - Missione 4 Istruzione e Ricerca - Componente C2 Investimento 1.1, Fondo per il Programma Nazionale di Ricerca e Progetti di Rilevante Interesse Nazionale (PRIN) funded by the European Commission under the NextGeneration EU programme, project “Advanced optimization METHODS for automated central vein Sign detection in multiple sclerosis from magnetic resonance imaging (AMETISTA)”, code: P2022J9SNP, MUR D.D. financing decree n. 1379 of 1st September 2023 (CUP E53D23017980001), project “Numerical Optimization with Adaptive Accuracy and Applications to Machine Learning”, code: 2022N3ZNAXMUR D.D. financing decree n. 973 of 30th June 2023 (CUP B53D23012670006), and by Partenariato esteso FAIR “Future Artificial Intelligence Research” SPOKE 1 Human-Centered AI. Obiettivo 4, Project “Mathematical and Physical approaches to innovative Machine Learning technologies (MaPLe)”.

## Competing interests declarations

The authors have no relevant interests to disclose.

## Data availability statements

The datasets utilized in this research are publicly accessible and commonly employed benchmarks in the field of Machine Learning and Deep Learning, see [36, 37].

## References

- [1] J. Barzilai, J. M. Borwein, Two-point step size gradient methods, *IMA journal of numerical analysis* 8 (1) (1988) 141–148. [doi:10.1093/imanum/8.1.141](https://doi.org/10.1093/imanum/8.1.141).
- [2] J. Nocedal, S. Wright, *Lecture notes*, Springer, Nature Switzerland, 2006. [doi:10.1007/978-0-387-40065-5](https://doi.org/10.1007/978-0-387-40065-5).
- [3] Y. Nesterov, *Lectures on convex optimization*, Springer, New York, NY, 2018. [doi:10.1007/978-3-319-91578-4](https://doi.org/10.1007/978-3-319-91578-4).

- [4] H. Robbins, M. S., A stochastic approximation method, *The Annals of Mathematical Statistics* 22 (1951) 1400–407. [doi:10.1214/AOMS/1177729586](https://doi.org/10.1214/AOMS/1177729586).
- [5] L. Bottou, Y. LeCun, Large scale online learning, in: *Neural Information Processing Systems*, Vol. 16, 2004, pp. 217–224, available at: [https://proceedings.neurips.cc/paper\\_files/paper/2003](https://proceedings.neurips.cc/paper_files/paper/2003).
- [6] L. Bottou, F. E. Curtis, J. Nocedal, Optimization methods for large-scale machine learning, *Siam Review* 60 (2) (2018) 223–311. [doi:10.1137/16M1080173](https://doi.org/10.1137/16M1080173).
- [7] F. E. Curtis, K. Scheinberg, R. Shi, A stochastic trust region algorithm based on careful step normalization, *Inform Journal on Optimization* 1 (3) (2019) 200–220. [doi:10.1287/ijoo.2018.0010](https://doi.org/10.1287/ijoo.2018.0010).
- [8] S. Bellavia, B. Morini, S. Rebegoldi, An investigation of stochastic trust-region based algorithms for finite-sum minimization, *Optimization Methods and Software* (2024) 1–30 [doi:10.1080/10556788.2024.2346834](https://doi.org/10.1080/10556788.2024.2346834).
- [9] F. E. Curtis, R. Shi, A fully stochastic second-order trust region method, *Optimization Methods and Software* 37 (3) (2022) 844–877. [doi:10.1080/10556788.2020.1852403](https://doi.org/10.1080/10556788.2020.1852403).
- [10] Y. Fang, S. Na, M. W. Mahoney, M. Kolar, Fully stochastic trust-region sequential quadratic programming for equality-constrained optimization problems, *SIAM Journal on Optimization* 34 (2) (2024) 2007–2037.
- [11] C. Tan, S. Ma, Y. Dai, Y. Qian, Barzilai-Borwein step size for stochastic gradient descent, in: *Neural Information Processing Systems*, 2016, available at: <https://dl.acm.org/doi/10.5555/3157096.3157173>.
- [12] L. Wang, H. Wu, I. Matveev, Stochastic gradient method with Barzilai-Borwein step for unconstrained nonlinear optimization, *Journal of Computer and Systems Sciences International* 60 (1) (2021) 75–86. [doi:10.1134/S106423072101010X](https://doi.org/10.1134/S106423072101010X).
- [13] J. Liang, Y. Xu, C. Bao, Y. Quan, H. Ji, Barzilai-Borwein-based adaptive learning rate for deep learning, *Pattern Recognition Letters* 128 (2019) 197–203. [doi:10.1016/j.patrec.2019.08.029](https://doi.org/10.1016/j.patrec.2019.08.029).

- [14] S. Bellavia, N. Krejić, N. K. Jerinkić, M. Raydan, SLiSeS: Subsampled line search spectral gradient method for finite sums, arXiv:2306.07379 (2023).
- [15] K. Natasa, K. J. Natasa, Spectral projected gradient method for stochastic optimization, *Journal of Global Optimization* 73 (2018) 59–81. doi:10.1007/s10898-018-0682-6.
- [16] A. S. Berahas, M. Takáč, A robust multi-batch L-BFGS method for machine learning, *Optimization Methods and Software* 35 (1) (2020) 191–219. doi:10.1080/10556788.2019.1658107.
- [17] R. Bollapragada, J. Nocedal, D. Mudigere, H.-J. Shi, P. T. P. Tang, A progressive batching L-BFGS method for machine learning, in: *International Conference on Machine Learning*, PMLR, 2018, pp. 620–629, available at: <https://proceedings.mlr.press/v80/>.
- [18] R. Gower, D. Goldfarb, P. Richtárik, Stochastic block BFGS: Squeezing more curvature out of data, in: *International Conference on Machine Learning*, PMLR, 2016, pp. 1869–1878, available at: <https://proceedings.mlr.press/v48/>.
- [19] A. Mokhtari, A. Ribeiro, Global convergence of online limited memory BFGS, *The Journal of Machine Learning Research* 16 (1) (2015) 3151–3181, available at: <https://www.jmlr.org/papers/v16/>.
- [20] X. Wang, S. Ma, D. Goldfarb, W. Liu, Stochastic quasi-Newton methods for nonconvex stochastic optimization, *SIAM Journal on Optimization* 27 (2) (2017) 927–956. doi:10.1137/15M1053141.
- [21] J. B. Erway, J. Griffin, R. F. Marcia, R. Omheni, Trust-region algorithms for training responses: machine learning methods using indefinite Hessian approximations, *Optimization Methods and Software* 35 (3) (2020) 460–487. doi:10.1080/10556788.2019.1624747.
- [22] M. Yousefi, Á. Martínez, Deep neural networks training by stochastic quasi-newton trust-region methods, *Algorithms* 16 (10) (2023) 490. doi:10.3390/a16100490.

- [23] R. Johnson, T. Zhang, Accelerating stochastic gradient descent using predictive variance reduction, in: *Neural Information Processing Systems*, Vol. 26, 2013, pp. 315–323, available at: [https://proceedings.neurips.cc/paper\\_files/paper/2013](https://proceedings.neurips.cc/paper_files/paper/2013).
- [24] Y. Dai, J. Yuan, Y.-X. Yuan, Modified two-point stepsize gradient methods for unconstrained optimization, *Computational Optimization and Applications* 22 (2002) 103–109. doi:10.1023/A:1014838419611.
- [25] R. Marcos, On the Barzilai and Borwein choice of steplength for the gradient method, *IMA J. Numerical Analysis* 13 (1993) 321–326. doi:10.1093/imanum/13.3.321.
- [26] E. G. Birgin, J. M. Martínez, M. Raydan, Spectral projected gradient methods: Review and perspectives, *Journal of Statistical Software* 60 (3) (2014) 1–21. doi:10.18637/jss.v060.i03.
- [27] D. Di Serafino, V. Ruggiero, G. Toraldo, L. Zanni, On the steplength selection in gradient methods for unconstrained optimization, *Applied Mathematics and Computation* 318 (2018) 176–195. doi:10.1016/j.amc.2017.07.037.
- [28] A. Conn, N. Gould, P. Toint, *Trust-region methods*, SIAM, Philadelphia, PA, 2000. doi:10.1137/1.9780898719857.
- [29] N. N. Schraudolph, J. Yu, S. Günter, A stochastic quasi-Newton method for online convex optimization, in: *Artificial intelligence and statistics*, *JMLR*, 2007, pp. 436–443, available at: <http://proceedings.mlr.press/v2/schraudolph07a.html>.
- [30] Y.-H. Dai, W. W. Hager, K. Schittkowski, H. Zhang, The cyclic Barzilai-Borwein method for unconstrained optimization, *IMA Journal of Numerical Analysis* 26 (3) (2021) 604–627. doi:https://10.1093/imanum/dr1006.
- [31] D. P. Kingma, J. Ba, Adam: A method for stochastic optimization, in: *3rd International Conference on Learning Representations, ICLR 2015 - Conference Track Proceedings*, 2015, available at: <http://arxiv.org/abs/1412.6980>.

- [32] R. H. Byrd, S. L. Hansen, J. Nocedal, Y. Singer, A stochastic quasi-Newton method for large-scale optimization, *SIAM Journal on Optimization* 26 (2) (2016) 1008–1031. doi:[10.1137/140954362](https://doi.org/10.1137/140954362).
- [33] J. Martens, New insights and perspectives on the natural gradient method, *The Journal of Machine Learning Research* 21 (1) (2020) 5776–5851, available at: <https://jmlr.org/papers/v21/17-678.html>.
- [34] N. S. Keskar, A. S. Berahas, adaQN: An adaptive quasi-newton algorithm for training RNNs, in: *Machine Learning and Knowledge Discovery in Databases*, Springer, 2016, pp. 1–16. doi:[10.1007/978-3-319-46128-1\\_1](https://doi.org/10.1007/978-3-319-46128-1_1).
- [35] J. d. Faria, R. Assunção, F. Murai, Fisher scoring method for neural networks optimization, in: *International Conference on Data Mining (SDM)*, SIAM, 2023, pp. 748–756. doi:[10.1137/1.9781611977653.ch84](https://doi.org/10.1137/1.9781611977653.ch84).
- [36] C.-C. Chang, C.-J. Lin, LIBSVM: a library for support vector machines, *Transactions on Intelligent Systems and Technology* 2 (3) (2011) 1–27. doi:[10.1145/1961189.1961199](https://doi.org/10.1145/1961189.1961199).  
URL <https://www.csie.ntu.edu.tw/~cjlin/libsvm/>
- [37] L. Deng, The MNIST database of handwritten digit images for machine learning research, *IEEE signal processing magazine* 29 (6) (2012) 141–142. doi:[10.1109/MSP.2012.2211477](https://doi.org/10.1109/MSP.2012.2211477).  
URL <https://yann.lecun.com/exdb/mnist/>
- [38] A. Krizhevsky, G. Hinton, Learning multiple layers of features from tiny images, Tech. rep., University of Toronto (2009).  
URL <https://www.cs.toronto.edu/~kriz/learning-features-2009-TR.pdf>
- [39] N. Krejić, N. Krklec Jerinkić, Á. Martínez, M. Yousefi, A non-monotone trust-region method with noisy oracles and additional sampling, *Computational Optimization and Applications* 89 (1) (2024) 247 – 278. doi:[10.1007/s10589-024-00580-w](https://doi.org/10.1007/s10589-024-00580-w).
- [40] X. Glorot, Y. Bengio, Understanding the difficulty of training deep feedforward neural networks, in: *Artificial intelligence and statistics*, JMLR, 2010, pp. 249–256, available at: <https://proceedings.mlr.press/v9/>.

- [41] G. Franchini, F. Porta, V. Ruggiero, I. Trombini, L. Zanni, Diagonal barzilai-borwein rules in stochastic gradient-like methods, in: International Conference on Optimization and Learning, Springer, 2023, pp. 21–35. [doi:10.1007/978-3-031-34020-8\\_2](https://doi.org/10.1007/978-3-031-34020-8_2).